Journal of Alzheimer's Disease 68 (2019) 809–837
DOI 10.3233/JAD-180707
IOS Press

Impaired Glucose Tolerance and Reduced Plasma Insulin Precede Decreased AKT Phosphorylation and GLUT3 Translocation in the Hippocampus of Old 3xTg-AD Mice

Chelsea M. Griffith[a,c], Lauren N. Macklin[a,c], Yan Cai[d,e], Andrew A. Sharp[a,b,c], Xiao-Xin Yan[d,e], Lawrence P. Reagan[f,g], April D. Strader[a,c,1], Gregory M. Rose[a,b,c] and Peter R. Patrylo[a,b,c,*]
[a]*Department of Physiology, Southern Illinois University School of Medicine, Carbondale, IL, USA*
[b]*Department of Anatomy, Southern Illinois University School of Medicine, Carbondale, IL, USA*
[c]*Center for Integrated Research in Cognitive and Neural Sciences, Southern Illinois University, Carbondale, IL, USA*
[d]*Department of Anatomy and Neurobiology, Central South University Xiangya School of Medicine, Changsha, Hunan, China*
[e]*Key Laboratory of Hunan Province in Neurodegenerative Disorders, Changsha, Hunan, China*
[f]*Department of Pharmacology, Physiology & Neuroscience, University of South Carolina, Columbia, SC, USA*
[g]*WJB Dorn Veterans Affairs Medical Center, Columbia, SC, USA*

Accepted 16 January 2019

Abstract.Several studies have demonstrated that mouse models of Alzheimer's disease (AD) can exhibit impaired peripheral glucose tolerance. Further, in the APP/PS1 mouse model, this is observed prior to the appearance of AD-related neuropathology (e.g., amyloid-β plaques; Aβ) or cognitive impairment. In the current study, we examined whether impaired glucose tolerance also preceded AD-like changes in the triple transgenic model of AD (3xTg-AD). Glucose tolerance testing (GTT), insulin ELISAs, and insulin tolerance testing (ITT) were performed at ages prior to (1–3 months and 6-8 months old) and post-pathology (16-18 months old). Additionally, we examined for altered insulin signaling in the hippocampus. Western blots were used to evaluate the two-primary insulin signaling pathways: PI3K/AKT and MAPK/ERK. Since the PI3K/AKT pathway affects several downstream targets associated with metabolism (e.g., GSK3, glucose transporters), western blots were used to examine possible alterations in the expression, translocation, or activation of these targets. We found that 3xTg-AD mice display impaired glucose tolerance as early as 1 month of age, concomitant with a decrease in plasma insulin levels well prior to the detection of plaques (∼14 months old), aggregates of hyperphosphorylated tau (∼18 months old), and cognitive decline (≥18 months old). These alterations in peripheral metabolism were seen at all time points examined. In comparison, PI3K/AKT, but not MAPK/ERK, signaling was altered in the hippocampus only in 18-20-month-old 3xTg-AD mice, a time point at which there was a reduction in GLUT3 translocation to the plasma membrane. Taken together, our results provide further evidence that disruptions in energy metabolism may represent a foundational step in the development of AD.

Keywords: 3xTg-AD, AKT, Alzheimer's disease, diabetes, glucose, GLUT, hippocampus, insulin, metabolism

INTRODUCTION

Alzheimer's disease (AD) is a neuropathological disorder characterized by amyloid-β plaques, neurofibrillary tangles, neuronal synapse and cell

[1]In memoriam.

*Correspondence to: Peter R. Patrylo, Southern Illinois University School of Medicine, Carbondale, IL 62901, USA. Tel.: +1 618 453 6743; E-mail: ppatrylo@siumed.edu.

loss, and profound memory impairment that eventually results in dementia. Two important risk factors for developing AD are aging and diabetes, both conditions associated with peripheral metabolic alterations. Humans with diabetes are more likely to have cognitive impairment [1–6] and although animal models of diabetes do not develop the characteristic plaques and tangles, they have been shown to exhibit AD-like changes such as increased amyloid-β (Aβ) protein levels and tau phosphorylation [7–10]. Further, pro-diabetic dietary or experimental manipulations (e.g., high fat diet or peripheral streptozotocin administration) can worsen AD-related neuropathology and/or cognitive performance in mouse models of AD [7, 10–16].

Peripheral metabolic alterations such as increased or decreased fasting insulin levels, decreased insulin response to glucose challenge, insulin resistance, or hyperglycemia that are not the result of a diagnosis of diabetes also positively correlate with cognitive decline and AD-related pathology in humans [16–20]. Recent studies have demonstrated that mouse models of AD can also exhibit reduced peripheral glucose tolerance [21–26] and that, at least in the APP/PS1 mouse model, this impairment occurs prior to AD-related neuropathology or cognitive decline [22]. Taken together, these data suggest that insulin and peripheral glucose dysregulation may play a role in AD pathogenesis.

In the current study we examined the relationship between alterations in peripheral glucose tolerance and the appearance of AD-like neuropathology and cognitive deficits in the 3xTg-AD mouse model. Glucose tolerance testing (GTT), insulin ELISAs, and insulin tolerance testing (ITT) were performed at ages prior to (1–3 months and 8–10 months old) and after (16-18 months old) neuropathology was detected. Furthermore, we evaluated whether there was an age-related change in insulin signaling in the hippocampus, a brain structure that plays a key role in explicit learning and memory (e.g., spatial learning and memory). Western blots were used to examine the two-primary insulin signaling pathways, PI3K/AKT and MAPK/ERK, at multiple time points. Finally, since several of the downstream players in the PI3K/AKT pathway are associated with metabolism (e.g., GSK3, glucose transporters), western blots were also used to assess whether, and when, alterations in the expression, translocation or activation of these targets could be occurring and thus contribute to AD-related pathogenesis and cognitive decline.

MATERIALS AND METHODS

Animals

Male 3xTg-AD mice and age-matched wild type controls on a C57BL/6J-129S1/SvlmJ background were used for all experiments. With the exception of some of the metabolic studies (described below), separate groups of animals were used for each component (total animal number: 3xTg-AD = 192, wild type = 191; Neuroanatomy: 3xTg-AD = 25, wild type = 25; Behavior: 3xTg-AD = 79, wild type = 75; Metabolism: 3xTg-AD = 50, wild type = 51; Pancreas anatomy: 3xTg-AD = 10, wild type = 10; Westerns: 3xTg-AD = 28, wild type = 30). The 3xTg-AD mouse was created using a Thy1.2 promoter to express human mutated APP and hyperphosphorylated tau primarily in the CNS. These mice were then mated to a PS1 mutant line to create the triple mutant model of AD [27]. Animals were bred and housed in the Southern Illinois University Carbondale (SIUC) vivarium on a 12-h/12-h light dark cycle and were provided Purina rodent chow (fat: 13.5%, protein: 28.5%, carbohydrates: 58%) and water *ad libitum*. All experiments were approved by SIUC's Institutional Animal Care and Use Committee and comply with the guidelines set forth by the National Institutes of Health.

Neuroanatomy

Immunohistochemistry (IHC) was used to examine Aβ accumulation and tau hyperphosphorylation. Briefly, mice ($n = 5$/age/genotype: 1-2, 4–6, 8–10, 14, 18 months; $n = 25$ 3xTg-AD and 25 wild type) were anesthetized with an intraperitoneal (ip) injection of pentobarbital (100 mg/kg) and then intracardially perfused with 4% paraformaldehyde. Following perfusion, brains were extracted, post-fixed overnight and cryoprotected in 30% sucrose. Coronal sections were cut at 35-μm thickness using a cryostat. To quench endogenous peroxidase activity, sections were treated with 1% H_2O_2 in 10 mM phosphate-buffered saline (PBS, pH 7.4) for 30 min. For Aβ labeling, sections underwent antigen retrieval in 50% formic acid in PBS at room temperature 30 min prior to quenching of the endogenous peroxidase activity. Sections were then blocked in 5% normal goat or horse serum in PBS with 0.3% Triton X-100 for 1 h, after which they were incubated with primary antibodies (see Table 1) in blocking serum overnight (4°C). The next day, sections were rinsed and reacted

Table 1
Antibodies used in this study

Antibody	Source	Dilution
For Immunohistochemistry:		
6E10 (anti-Aβ)	Signet, Dedham, MA	1:3000
Ter42 (anti-Aβ 37-42)	Chemicon, Temecula, CA	1:2000
Phospho-Tau (PHF) (Ser202/Thr205)	ThermoFisher Scientific, Waltham, MA	1:3000
Insulin	Sigma-Aldrich, St. Louis, MO	1:200
For Western Blotting:		
p44/42 MAPK	Cell Signaling Technology, Danvers, MA	1:1000
Phospho-p44/42 MAPK (Thr202/Tyr204)	Cell Signaling Technology, Danvers, MA	1:1000
IRS-1	Abcam, Cambridge, MA	1:500
Phospho-IRS-1 (Ser307)	Cell Signaling Technology, Danvers, MA	1:1000
AKT	Rockland, Gilbertsville, PA	1:2500
Phospho-AKT (Ser473)	Cell Signaling Technology, Danvers, MA	1:2000
GSK3α/β	Cell Signaling Technology, Danvers, MA	1:1000
Phospho-GSK3α/β (Ser21/9)	Cell Signaling Technology, Danvers, MA	1:1000
Phospho-Tau PHF (Ser202/Thr205)	ThermoFisher Scientific, Waltham, MA	1:500
Phospho-Tau (Ser396)	Cell Signaling Technology, Danvers, MA	1:1000
GLUT3	Alpha Diagnostic, San Antonio, TX	1:2500
GLUT 4	Dr. Lawrence Reagan	1:500
β-Actin	Sigma-Aldrich, St. Louis, MO	1:10,000
GAPDH	Genetex, Irvine, CA	1:5000

with biotinylated goat anti-rabbit or horse anti-mouse IgGs for 2 h (1:400) followed by the Vectastain elite ABC kit (Vector Laboratories; Burlingame, CA) for another hour. Immunoreactive product was visualized using 0.003% H_2O_2, 0.05% DAB, with or without enhancement (0.025% $NiCl_2$ or 0.025% $CoCl_2$). Three 10-min washes with PBS with 1% Triton-X100 were performed between all incubations. Sections were mounted on microscope slides, air-dried, delipidated in a series of ethanol and xylene and then cover slipped.

Behavioral testing: Morris water maze

Cognitive function was evaluated in 3xTg-AD and wild type mice using the Morris water maze (6–10 months $n = 23$ 3xTg-AD, 16 wild type; 14–16 months $n = 25$ 3xTg-AD, 25 wild type; $\geq$18 months $n = 31$ 3xTg-AD, 34 wild type). The pool consisted of a circular tank (1.35 m diameter) painted white and filled with water made opaque by the addition of non-toxic white tempera paint. Water temperature was maintained at approximately 21.5°C. For the hidden platform task, a square hidden platform (10 × 10 cm) was located in the "center" of one quadrant of the maze and submerged approximately 0.5 cm below the surface of the water. For the visible platform task, an extension was added to the hidden platform so that the location of the platform was clearly visible above the water level. The four walls of the testing room were decorated with distinct visual cues to clearly differentiate between them. The protocol involved first testing the mice for 3 days (3 trials/day, different starting position for each trial, 30-min inter-trial interval) in the visible platform task to ensure that all animals used were comparable in vision, anxiety and motivation. Outliers from the visible platform task were excluded from further training. Next, animals were tested using the hidden platform task with a 15 trial over 5-day protocol (three trials/day with 30 min inter-trial intervals; 90 s maximum trial duration). The latency to find the hidden platform was measured using an overhead camera with digital tracking software (AnyMaze, San Diego Instruments; San Diego, CA). One day following the hidden platform training, the mice were given a probe trial. This consisted of a single 60-s trial with the platform removed from the pool. The latency to first crossing of the place where the platform had been located and the total number of crossings during the entire probe trial were compared between groups at each age point examined.

Intraperitoneal Glucose Tolerance Test (ipGTT)

Peripheral metabolic profile was assessed in 3xTg-AD and wild type controls using ipGTTs and ipITTs ($n = 50$ 3xTg-AD mice total; 51 wild type total). Prior to the ipGTT the animals were fasted for 12 hours. Subsequently, mice were given an ip glucose injection (20% D-glucose in PBS at 1.5 g/kg

body weight). Plasma glucose readings were taken in duplicate at 0, 15, 30, 45, 60, and 120 min post-glucose injection by obtaining a blood sample from a tail prick (1.0–1.5 μl). A human OTC glucometer (TRUEtrack, Nipro Diagnostics, Fort Lauderdale, FL) was used to measure blood glucose levels. About 500 μl of blood was also collected at baseline (time 0) and 15 min post-glucose injection to examine plasma insulin levels. To measure insulin concentrations, an Ultra-Sensitive Rat Insulin ELISA kit (Chrystal Chem, Downer's Grove, IL) was used following the instructions provided by the supplier. Blood samples contaminated with lysed red blood cells were excluded from analysis. Insulin ELISA readings were obtained using a Multiskan Plus plate reader (Thermo Fisher Scientific; Grand Island, NY) with filters set at 450 nm and 620 nm wavelengths.

Intraperitoneal Insulin Tolerance Test (ipITT)

When possible, separate groups of mice were used for ipGTTs and ipITTs. When the same mice were used for both ipGTTs and ipITTs, 1-2 weeks were allotted between the ipGTT and the ipITT. This was primary done for the eldest age group examined (17-18 months old). For ipITTs, mice were assessed for changes in insulin sensitivity using an ip injection of insulin (0.25 U/kg body weight, Humulin-R; Lilly Research Labs, Indianapolis, IN). Blood samples were taken in duplicate at time point 0 (pre-injection) and post-injection time points 15, 30, 45, and 60 min. For these experiments, the mice were fasted for 5 h prior to insulin injection.

Pancreatic analysis

3xTg-AD mice and wild type controls at 2-3 and 8–10 months of age were used to assess whether islet size or insulin immunoreactivity differed between groups ($n = 5$ mice/genotype/age). Histochemical staining with hematoxylin and eosin (H&E) was used to examine islet size, while IHC was used to assess insulin staining within islets. Following a 5-h fast, animals were terminally anesthetized using sodium pentobarbital (100 mg/kg body weight, ip) and pancreatic tissue was dissected out and placed in Bouin's fixative overnight. The tissue was then transferred to a 70% ethanol solution and kept at 4°C until paraffin embedding. Sections were cut at 5 microns and mounted onto microscope slides.

Prior to staining the slides were placed in an oven at 60–80°C to melt the paraffin, then placed in Histoclear for 2 min (agitating the slide rack for the first 10 s) and subsequently transferred to two additional solutions of Histoclear for 2 min each to remove the paraffin. After this, the tissue was washed three times in 100% ethanol (2 min/wash) followed by a wash in 95% ethanol for 2 min. The slides were then transferred to distilled water. For H&E staining, sections were first placed in hematoxylin for 4 min, rinsed in distilled water and decolorized in 2 rinses of acid alcohol until they appeared brick red, and then rinsed again. The slides were subsequently placed in lithium carbonate (1 min) followed by distilled water for an additional minute. Next, the slides were transferred to the eosin stain and agitated for 5–15 s followed by a rinse with distilled water. The tissue was then dehydrated in three changes of 100% isopropyl alcohol, cleared and coverslipped using Clearium mounting medium (Leica Biosystems).

For IHC, sections were blocked in normal horse serum at 23°C for 1 h. Next, sections were incubated in the anti-insulin primary antibody overnight at 4°C. Sections were then washed twice with Tris buffer (pH 7.2; 5 min/wash) and reacted with mouse-anti-mouse IgG secondary antibody (1:400; Vector Laboratories, Burlingame, CA) for 30 min, followed by another two washes with Tris buffer. Lastly, sections were incubated in ABC complex and prepared for viewing as has been previously described.

Analysis of islet area in 3xTg-AD versus wild type control mice was performed using Image J software (NIH) with 3 slides used per animal (approximately 300 microns between each examined slide to make sure that the same islet was not analyzed twice). Each slide had sections containing the head, body and tail regions of the pancreas. For each slide, 10 islet photographs were obtained by randomly scanning through the entire slide and taking a picture of the first islet that came into view. After the first islet was found, the field of view was moved between 300 and 500 microns. If an islet was not present, scanning would continue until an islet was found. Images were then imported into Image J where the entire islet was outlined and an area measurement was obtained.

Analysis of the optical density (OD) of islet insulin-immunoreactivity was also performed using Image J analysis using a similar randomized procedure. Images were imported into Adobe Photoshop, converted into grey scale pictures and imported into Image J. Each collected islet was analyzed for insulin

immunoreactivity by determining the OD of insulin in the islet itself. Background OD was subtracted from islet OD to normalize staining across images.

Western blots

Mice were overdosed with pentobarbital (100 mg/kg, ip) and their brains were extracted ($n = 28$ 3xTg-AD mice, 30 wild type mice total). Hippocampi were collected, frozen on dry ice, and then stored at –80°C until use. Samples were prepared using a modified version of a protocol described by Reagan and colleagues [28, 29]. Briefly, samples were homogenized in 700 µl of cold homogenization buffer (0.32 M sucrose, 2 mM EDTA, 2 mM EGTA, 20 mM HEPES, and protease and phosphatase inhibitors) and centrifuged at 800× *g* for 10 min. The supernatant was saved and used to examine levels of insulin signaling proteins as well as the total levels of the glucose transporters GLUT3 and GLUT4. A portion of this fraction was further centrifuged at 16,000× *g* for 30 min at 4°C. The resulting pellet, which contained the plasma membrane fraction, was re-suspended in PBS with protease and phosphatase inhibitors to assess GLUT translocation. Protein concentrations were determined using a bicinchoninic assay kit (Pierce, Thermo Fisher Scientific; Grand Island, NY). Prior to gel loading, total fraction samples were heated at 95°C for 5 min; samples used to evaluate plasma membrane proteins were not heated. Protein was loaded and resolved onto 7.5% or 10% SDS-PAGE gels, transferred to polyvinylidene fluoride (PVDF) membranes and then probed with primary antibody. (See Table 1 for antibody information.) For total samples, β-actin was used as the loading control. For glucose transporter experiments, GAPDH was used as the control protein to normalize total samples and verify successful isolation of the plasma membrane fraction. Plasma membrane samples were normalized to total samples. Appropriate fluorescent secondary antibodies (1:10,000; goat anti-mouse 700 and goat anti-rabbit 800; Rockland Immunochemicals Inc., Limerick, PA) were used for densitometric quantification of protein bands using the Odyssey LI-COR system (LI-COR Biotechnology; Lincoln, NE).

Microscopy

All tissue sections were analyzed by light microscopy using a Zeiss Axioimager (Zeiss; Oberkochen, Germany). Images from wild type and 3xTg-AD sections were taken at the same exposure.

Statistical analysis

All data are presented as mean ± SEM. Repeated measures ANOVA (RM ANOVA; Graph Pad Prism, Version 5) was used to analyze behavioral data (i.e., visible and hidden platform trials) with Bonferroni *post-hoc* analysis where appropriate. Probe data were compared between groups using Student's *t*-tests. Differences in glucose tolerance and insulin sensitivity between 3xTg-AD mice and controls were also compared using RM ANOVA with Bonferroni *post-hoc* tests used to assess significance at specific time-points on the ipGTT and ipITT curves. Trapezoidal analysis was used to calculate the area under the curve (AUC) for ipGTTs; these values were subsequently compared between groups using a Student's *t*-test. Student's *t*-tests were used to compare insulin levels at baseline and 15 min post-glucose bolus between groups at each age examined. Average pancreatic islet area and average insulin intensity were analyzed using a Student's *t*-test for each age group. Differences between means for the western blot experiments were analyzed using Student's *t*-tests using Welch's correction for groups with unequal variance. For all experiments, statistical significance was defined as $p < 0.05$.

RESULTS

Neuroanatomy

The development of Aβ and tau pathologies in 3xTg-AD mice has been described in previous studies [27]. In general, labeling of neuronal somata by selected domain and p-Tau antibodies are detectable in the cerebral cortex and hippocampus as early as 3 weeks of age [30] while extracellular amyloid-containing plaques in the forebrain appear around 12–14 months of age [31]. Overall, the progression of this pathology in the mice in our colony is consistent with existing literature, as illustrated using three different antibodies: 6E10 ($A\beta_{40}$, $A\beta_{42}$, and AβPP), Ter 42 ($A\beta_{1\text{-}42}$) and Phospho-Tau PHF (Ser202/Thr205) (Fig. 1). In mice from our colony it appears that, at 1-2 months of age, 3xTg-AD mice show intraneuronal 6E10 staining in pyramidal neurons in cortical layer V, the subiculum, and hippocampal region CA1 (Fig. 1A). However, extracellular 6E10 or $A\beta_{1\text{-}42}$

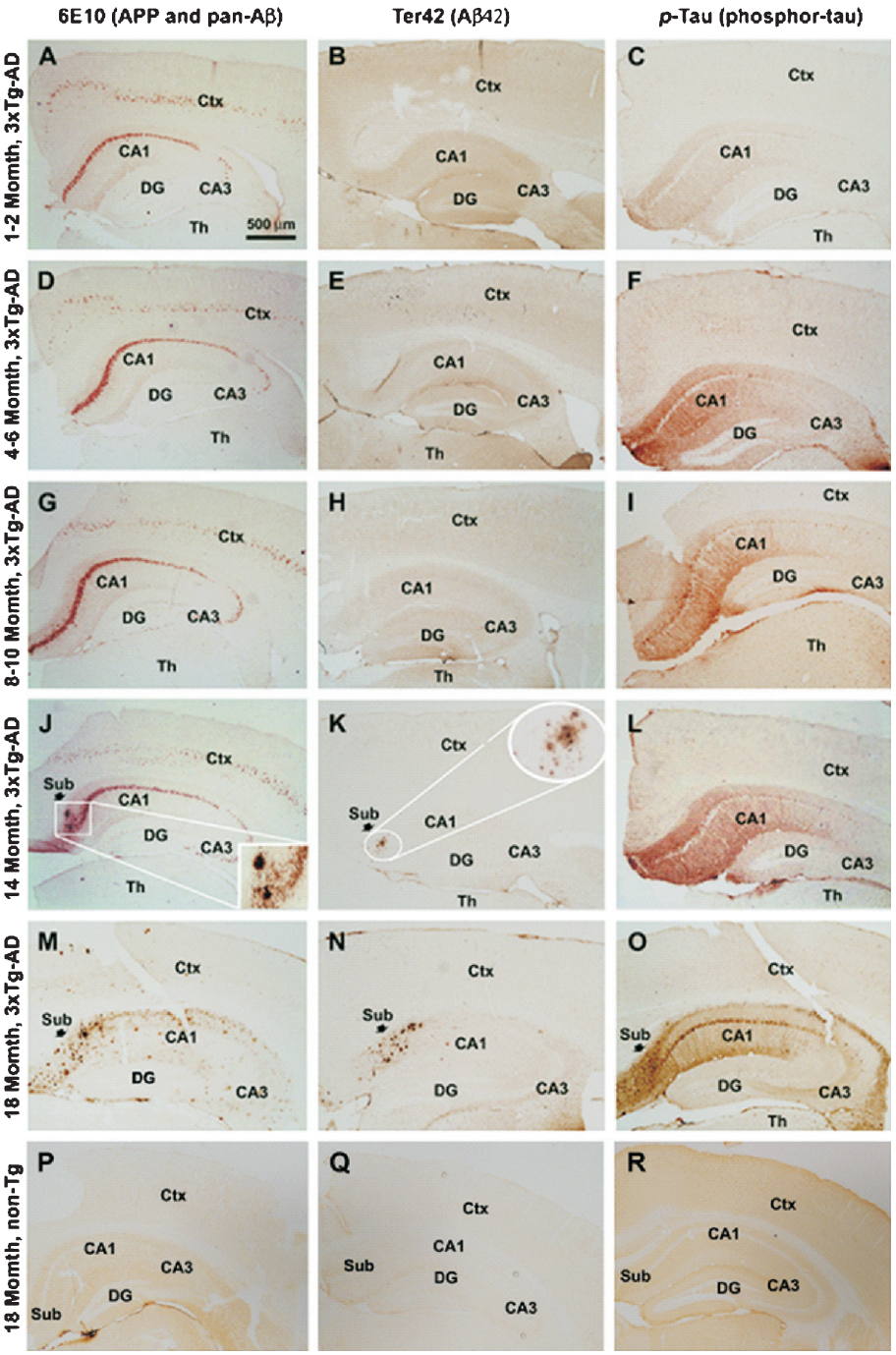

Fig. 1. Human amyloid precursor protein (APP), amyloid-β peptide 1–42 (Aβ), and human hyper-phosphorylated tau (p-Tau) immunoreactivities in the forebrain of 3xTg-AD mice at 1-2, 4–6, 8–10, 14, and 18 months of age. In wild type control mice, no immunoreactivity for any of these epitopes was detected at any age group examined. (P-R show examples from a representative 18-month-old wild type mouse). In comparison, 3xTg-AD mice exhibited intraneuronal 6E10 and p-Tau staining in pyramidal neurons in the subiculum, and hippocampal region CA1 in 1-2-month-old mice (A, C) that further increased with age. However, extracellular 6E10 or $A\beta_{1-42}$ immunoreactivity (plaque-like deposits) was not observed until 14 months of age (J, K). Insets in J and K show plaques at higher magnification. By 18 months of age, 3xTg-AD mice exhibited extracellular plaques with 6E10 and $A\beta_{1-42}$ immunohistochemistry (M, N). P-tau immunoreactivity was also highly visible in the principal neurons of the subiculum and CA1 in 18-month-old 3xTg-AD mice (O). Scale bar in A applies to all other images. Ctx, neocortex; DG, dentate gyrus; Sub, subiculum; Th, thalamus.

immunoreactivity were not observed (Fig. 1A and B, respectively; age of animal shown = 2 months). In addition, very little p-Tau immunoreactivity was seen in the somata or processes of pyramidal neurons in hippocampal region CA1 (Fig. 1C). Identical sections from age-matched wild type controls exhibited no staining for any of these antibodies (data not shown). Similar patterns of 6E10 and Ter42 were observed at 4–6 (Fig. 1D, E; age of animal shown = 6 months) and 8–10 months of age (Fig. 1G, H; age of animal shown = 10 months), although p-Tau immunoreactivity was increased in these age groups (Fig. 1F, I). By 14 months of age, 3xTg-AD mice exhibited extracellular plaques with 6E10 (Fig. 1J) and Ter42 (Fig. 1K). Labeled plaques were increased, particularly in the subiculum, in 18-month-old 3xTg-AD mice (Fig. 1M, N). Additionally, by 18 months of age p-Tau immunoreactivity was highly visible in the principal neurons of the subiculum and CA1 (Fig. 1O). In contrast, sections from 18-month-old wild type controls exhibited no staining for any of these antibodies (Fig. 1P-R).

Behavioral testing: Morris water maze

Learning and memory were evaluated using the Morris water maze. Prior to hidden platform training, mice were evaluated using the visual platform test to rule out possible differences in visual acuity, swimming ability and motivation. Both wild type and 3xTg-AD mice at 6–10 and 14–16 months of age performed similarly on the visible platform task suggesting that blindness, swimming ability and motivation were not potential confounds (6–10 months: 3xTg-AD $n = 23$; wild type $n = 16$; 14–16 months: 3xTg-AD $n = 25$; wild type $n = 25$; data not shown). However, amongst the oldest age group examined ($\geq$18 months: 3xTg-AD $n = 31$; wild type $n = 34$) some animals failed the visual platform (3xTg-AD = 9 mice, wild type = 3 mice) and were thus excluded from further testing. This failure on the visual platform could reflect an aging-related decline in visual acuity in both genotypes, potentially compounded by amyloid deposition in the retina of the transgenic mice [32, 33].

As shown in Fig. 2A, 6-10-month-old 3xTg-AD mice and wild type controls exhibited comparable reductions in the latency to find the platform during the five days of hidden platform training (RM ANOVA: time $p < 0.0001$; genotype $p > 0.2$; interaction $p > 0.25$). To test memory retention, a probe trial was performed one day after the last hidden platform test. No statistically significant differences were found between 3xTg-AD mice and controls in the number of platform location crossings (3xTg-AD = 4.7 ± 0.9; WT = 4.3 ± 0.92; $p > 0.7$, *t*-test) or the latency to the first platform location crossing (3xTg-AD = 9 ± 3.16 s; WT = 19.8 ± 5.25 s; $p > 0.07$, *t*-test) (Fig. 2A, right). Taken together, these data show that young adult 3xTg-AD mice and controls can both learn and remember the location of the hidden platform in the water maze task.

However, by 14–16 months of age a difference was detectable between 3xTg-AD mice and their age matched wild type controls. Specifically, as shown in Fig. 2B, 3xTg-AD mice exhibited a slower rate of learning compared to controls during the five days of MWM training, although by day five both groups showed a comparable reduction in the latency to find the hidden platform (RM ANOVA: time $p < 0.0001$; genotype $p < 0.01$; interaction $p > 0.14$). In addition, probe testing revealed no statistically significant differences between groups in the number of platform crossings (3xTg-AD = 4.3 ± 0.5; WT = 4.5 ± 0.5; $p > 0.7$) or the latency to the first platform crossing (3xTg-AD = 12.9 ± 3.1 s; WT = 11.4 ± 2.4 s; $p = 0.7$) (Fig. 2B, right), indicating that memory retention was preserved in 14-16-month-old 3xTg-AD mice.

In contrast to mice at younger ages, 3xTg-AD mice $\geq$18 months of age showed clear impairment compared to their wild type counterparts. Specifically, while both groups exhibited a reduction in the latency to the hidden platform during the five days of training (RM ANOVA: time $p < 0.0001$), 3xTg-AD mice were not as efficient in finding the platform on the last two days (RM ANOVA: genotype $p < 0.006$; interaction $p < 0.004$; Fig. 2C). Further, during the probe test, aged 3xTg-AD mice made significantly fewer platform location crosses (3xTg-AD = 2.3 ± 0.7; WT = 4.25 ± 0.6; $p < 0.04$) and had a significantly longer latency to the first platform location cross (3xTg-AD = 30.29 ± 6.6 s; WT = 12.63 ± 2.33 s; $p < 0.007$) (Fig. 2C, right). Taken together, these data suggest that by 18 months of age, 3xTg-AD mice have impaired spatial learning and memory compared to age-matched wild type controls.

Glucose tolerance test

After establishing the time course of pathogenesis and cognitive decline in our 3xTg-AD mice, we examined the potential relationship of changes in glucose regulation to these processes.

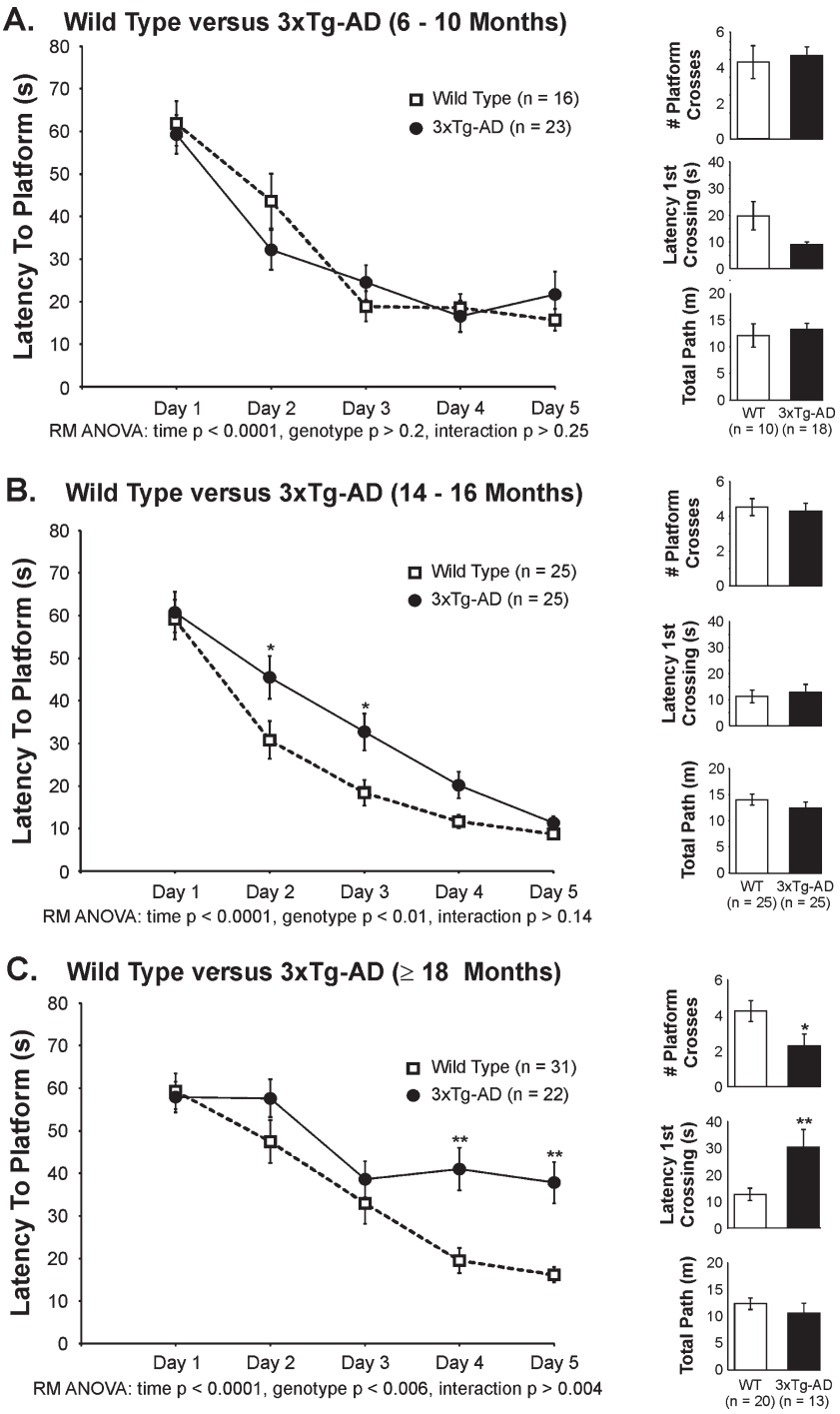

Fig. 2. Morris water maze data from 6–10 (A), 14–16 (B), and ≥18-month-old (C) 3xTg-AD and wild type control mice. Left - Latency to find the hidden platform over the 5-day training period. No difference was observed in 6-10-month-old 3xTg-AD mice compared to controls. By 14–16 months of age, a difference rate of learning was noted, although by the 5th day of training similar latencies to the hidden platform were observed in both groups. In contrast, the latency to find the hidden platform was significantly increased on days 4 and 5 in 3xTg-AD mice ≥18 months of age. Right: Probe data revealed a significant decrease in the number of platform location crosses and an increased latency to the first probe crossing in 3xTg-AD mice at ≥18 months of age compared to controls, but not earlier. $^{*}p<0.05$; $^{**}p<0.01$ versus wild type values.

Blood glucose levels were measured following an overnight fast and mice were subsequently subjected to an ipGTT. At 1–3 months of age 3xTg-AD mice exhibited elevated fasting glucose levels compared to controls (86.92 ± 3.92 mg/dL versus 76.23 ± 3.19 mg/dL; $p = 0.04$) and impaired glucose tolerance after an ip bolus of glucose (Fig. 3A; RM ANOVA: time $p < 0.0001$; genotype $p < 0.0001$; interaction: $p < 0.0001$). Further, the area under the curve measurement (AUC) calculated for the GTTs was significantly greater in 3xTg-AD mice (3xTg-AD 19,278 ± 1,525, WT 11,196 ± 899.3; $p < 0.0001$). At later ages (8–10 and 17-18 months old) no significant difference in fasting blood glucose levels between 3xTg-AD and wild type mice was observed (8–10 months: 3xTg-AD = 117.19 ± 9.56 mg/dL, WT = 98 ± 7.9 mg/dL, $p = 0.14$; 17-18 months: 3xTg-AD = 98.61 ± 7.95 mg/dL, WT = 87.9 ± 9, $p = 0.39$), although a similar disruption in glucose tolerance following a glucose challenge was found in 3xTg-AD mice at both 8–10 months (Fig. 3B; time $p < 0.0001$, genotype $p = 0.0039$, interaction: $p = 0.046$) and 17-18 months of age (Fig. 3C; time $p < 0.0001$, genotype $p < 0.005$, interaction $p < 0.0001$). In addition, the calculated AUC was greater in 3xTg-AD mice than in wild type controls at both time points (8–10 months: 3xTg-AD 24,497 ± 2,871, WT 16,965 ± 1,845, $p < 0.04$; 17-18 months: 3xTg-AD 11,722 ± 768, WT 6,335 ± 1,024, $p < 0.001$). Taken together, these data reveal that glucose tolerance, but not necessarily fasting blood glucose levels, was impaired in 3xTg-AD mice relative to wild type controls at all ages examined, thus demonstrating a lifelong dysfunction in glucose regulation in 3xTg-AD mice. In particular, glucose tolerance was impaired in 3xTg-AD mice at 1–3 months of age, well prior to Aβ plaque deposition, hyperphosphorylated tau accumulation or cognitive decline.

Plasma insulin levels and insulin sensitivity

To assess whether changes in insulin levels or secretion could contribute to the disruption of glucose tolerance in 3xTg-AD mice, blood plasma was collected during the ipGTTs prior to the glucose bolus at time point 0 (baseline) and at 15 min following the bolus. A significant decrease in fasting insulin levels was observed in 3xTg-AD mice, compared to wild type controls, at all ages examined (1–3 mo: 3xTg-AD 0.23 ± 0.04 ng/ml versus WT 0.35 ± 0.03 ng/ml, $p < 0.02$, Fig. 4A; 8–10 mo: 3xTg-AD 0.37 ± 0.07 ng/ml versus WT 1.05 ± 0.19 ng/ml, $p < 0.005$, Fig. 4B; 17-18 mo: 3xTg-AD 0.32 ± 0.06 ng/ml versus WT 1.20 ± 0.25 ng/ml, $p < 0.01$, Fig. 4C). Further, 3xTg-AD mice also showed significantly lower plasma insulin levels 15 min following the glucose bolus (1–3 mo: 3xTg-AD 0.28 ± 0.01 ng/ml versus WT 0.58 ± 0.03 ng/ml, $p < 0.00001$, Fig. 4A; 8–10 mo: 3xTg-AD 0.46 ± 0.03 ng/ml versus WT 1.64 ± 0.24 ng/ml, $p < 0.0003$, Fig. 4B; 17-18 mo: 3xTg-AD 0.87 ± 0.13 ng/ml versus WT 2.35 ± 0.25 ng/ml, $p < 0.0002$, Fig. 4C). Statistical analysis of the change in insulin levels over time (i.e., baseline versus 15 min post-glucose bolus) was not performed for the youngest age group since different animals were used for the two time points because we felt that the animals were too small to permit repeated collection of 500 μl samples. However, RM ANOVAs in the older mice showed that while both 3xTg-AD and control mice exhibited an increase in plasma insulin following the glucose bolus (Time: 8–10 mo, $p = 0.018$; 17-18 mo, $p < 0.0001$), the increase was significantly smaller in 3xTg-AD mice (genotype: 8–10 mo, $p = 0.0001$; 17-18 mo, $p = 0.0006$). Taken together, these data suggest that plasma insulin levels were decreased in 3xTg-AD mice and insulin secretion was diminished. These changes in glucose tolerance and plasma insulin levels in 3xTg-AD mice were not associated with a difference in weight, weight gain, or food intake in 3xTg-AD mice relative to controls (Table 2).

To assess whether the altered glucose tolerance observed in 3xTg-AD mice could also be the result of compromised insulin sensitivity, ipITTs were performed following 5 hours of fasting. Both 3xTg-AD and control mice exhibited a reduction in plasma glucose levels following an ip insulin bolus at all ages examined (Fig. 4D-F: Time: 1–3 mo $p < 0.0001$; 8–10 mo $p = 0.0012$; 17-18 mo $p = 0.008$; RM ANOVA), with no significant difference observed between groups (Genotype: $p > 0.05$ at all ages). These data suggest that insulin sensitivity appeared to be preserved in both 3xTg-AD and control mice.

Pancreatic analysis

To assess whether the reduction in insulin levels and secretion observed in 3xTg-AD mice could be a consequence of altered pancreatic morphology or biochemistry, stereological analysis of islet area and the intensity of insulin immunoreactivity (IR) was performed. As shown in Fig. 5, 3xTg-AD mice and wild type controls had similar distributions of islet area and average islet size at the two ages exam-

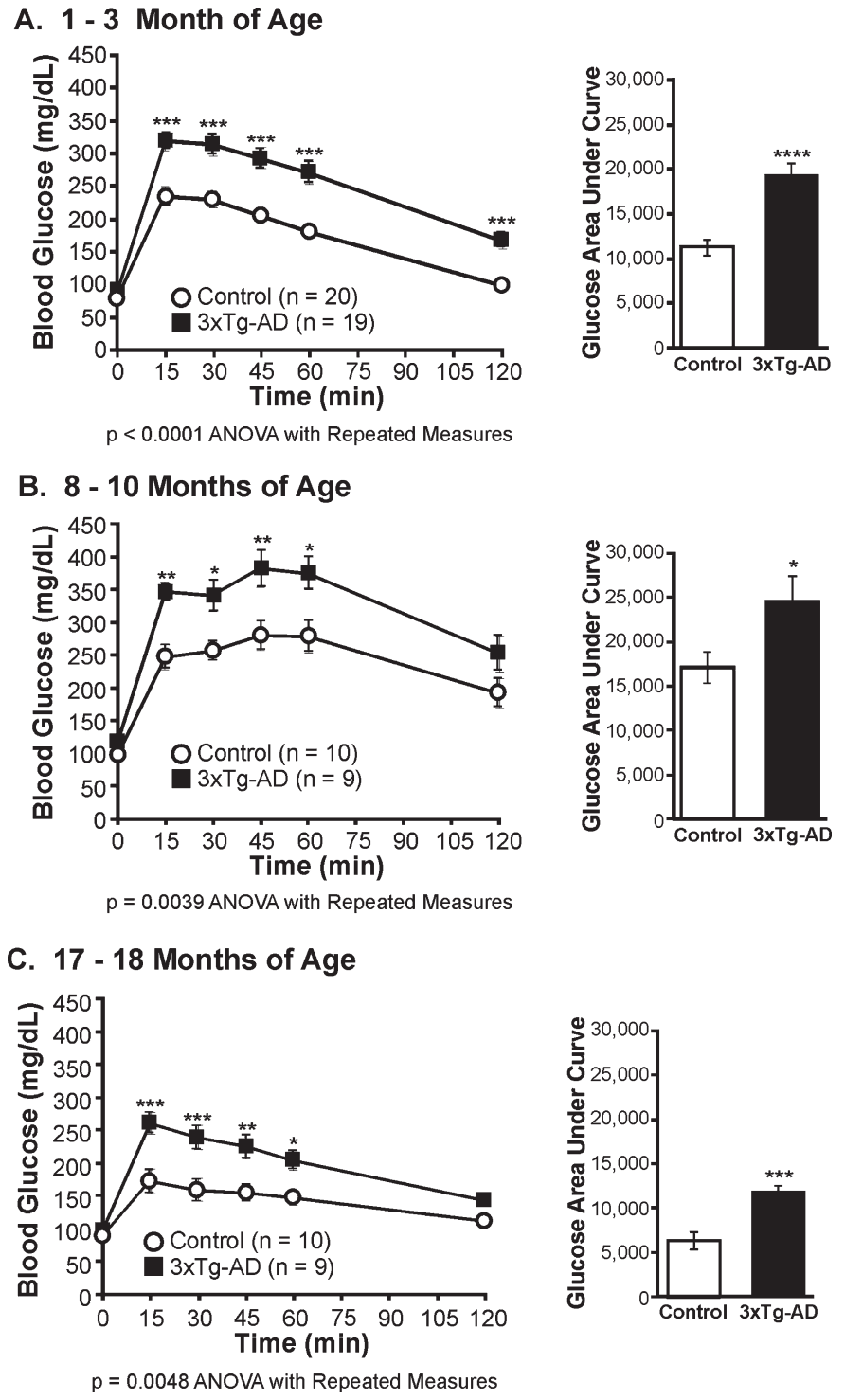

Fig. 3. 3xTg-AD mice exhibited impaired glucose regulation following an ip bolus of glucose at all ages examined: A) 1–3 months old; B) 8–10 months old; C) 17-18 months old. For each age group. the GTT time course is shown on the left and the integrated area under the curve (AUC) result is shown on the right. $^{*}p<0.05$, $^{**}p<0.01$, $^{***}p<0.001$, $^{****}p<0.0001$, versus control. See text for details of the statistical analysis.

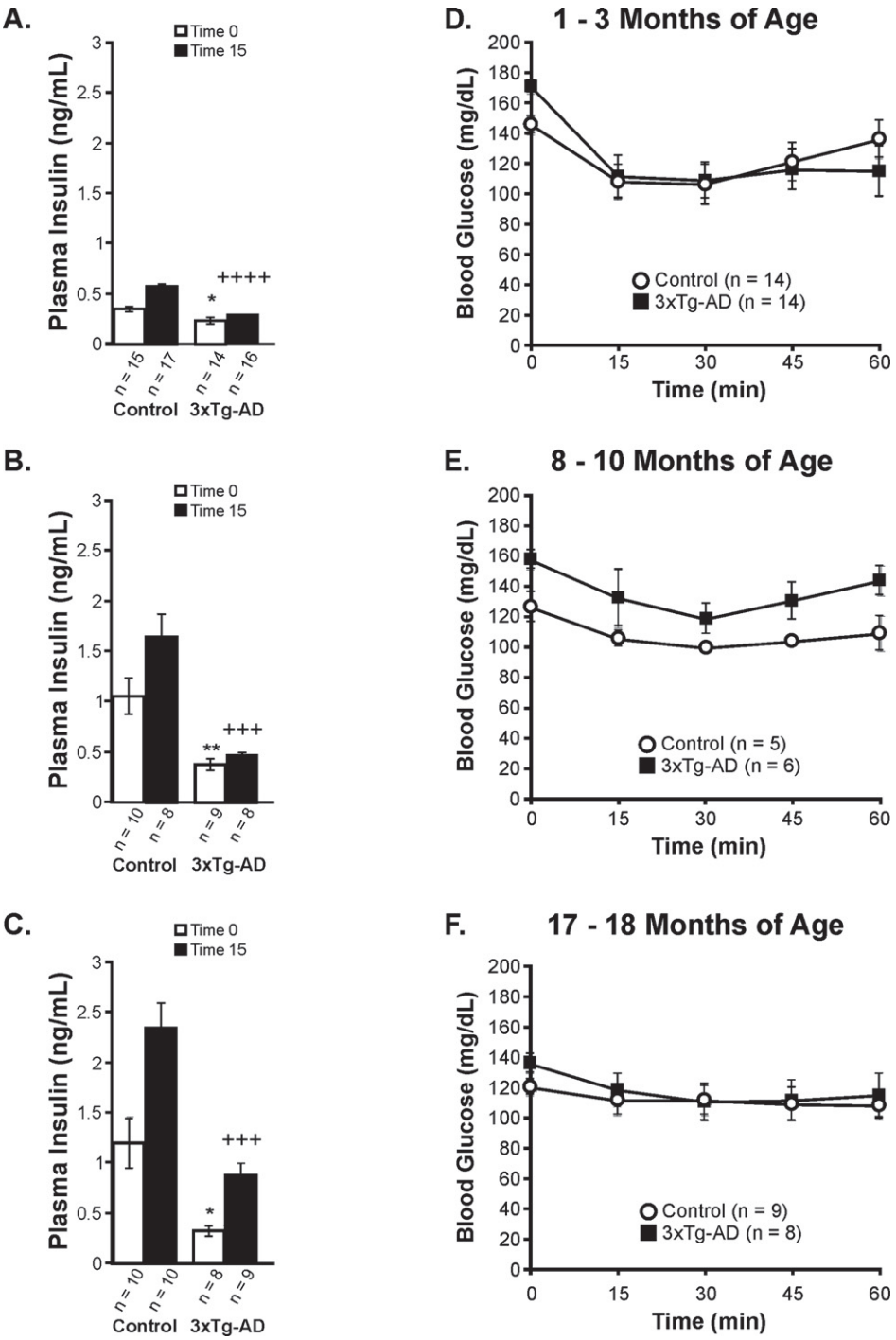

Fig. 4. A-C) Fasting insulin levels and post-glucose bolus insulin levels were decreased in the 3xTg-AD mice compared to controls suggesting alterations in insulin production and potentially secretion. Taken together these data suggest that glucose tolerance in impaired in 3xTg-AD mice may be due to a disruption in insulin production and secretion. $^{*}p < 0.05$, $^{**}p < 0.01$ 3xTg-AD versus control at Time 0; $^{+++}p < 0.001$, $^{++++}p < 0.0001$ versus control at Time 15. D-F) Following a bolus of ip insulin, both 3xTg-AD mice and age-matched wild type controls exhibited similar declines in plasma glucose levels at all ages examined. These results indicate that insulin sensitivity is not altered in 3xTg-AD mice relative to controls. See text for detailed statistical analysis.

Table 2
Body weight and food intake for the mice used in this study

	Average body weight over one week (grams)		Average food intake/day over one week (grams)	
	Wild Type	3xTg	Wild Type	3xTg
2-3 Months	22.55 ± 0.36	23.46 ± 0.45	4.21 ± 0.16	4.18 ± 0.15
4–6 Months	34.40 ± 0.83	35.36 ± 1.07	4.53 ± 0.30	4.21 ± 0.11
8–10 Months	37.42 ± 1.97	36.73 ± 0.89	4.37 ± 0.25	3.89 ± 0.13
17 Months	43.88 ± 1.82	42.05 ± 1.80	6.12 ± 0.45	5.19 ± 0.68

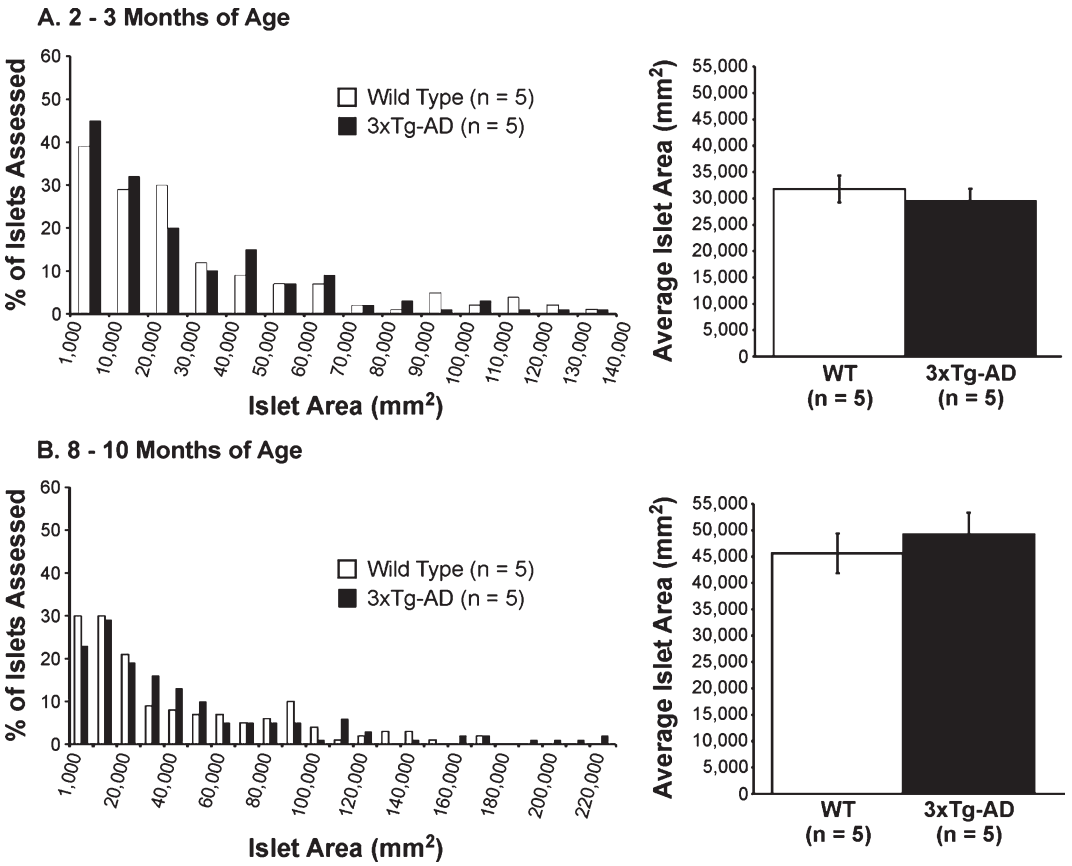

Fig. 5. Histogram illustrating pancreatic islet area measurements (graphs on left) and average islet area (graphs on right) for (A) 2-3-month-old and (B) 8-10-month-old 3xTg-AD and wild type control mice. Average islet area data is expressed as mean ± SEM and analyzed using a Student's *t*-test. There was no significant difference between genotypes in average islet area.

ined (2-3 months: 3xTg-AD 29,563 ± 2291 μm^2, WT 31,797 ± 2551 μm^2; 8–10 months 3xTg-AD 49,297 ± 4,033 μm^2, WT 45,630 ± 3,757 μm^2). In both wild type and 3xTg-AD mice there were comparable increases in islet area with age (compare upper and lower bar graphs in Fig. 5, right). In contrast to pancreatic islet number, the intensity of islet insulin immunoreactivity was significantly decreased in 3xTg-AD mice compared to wild type controls at both ages examined (2-3 months: 3xTg-AD 168.38 ± 1.91 OD, WT 177.12 ± 1.81 OD, $p = 0.002$; 8–10 months: 3xTg-AD 178.14 ± 2.12 OD, WT 189.12 ± 1.51 OD; $p < 0.0001$). Intensity histograms, bar graphs of mean values, and images of islet staining are shown in Fig. 6.

MAPK/ERK signaling is not changed in the 3xTg-AD mouse hippocampus

To determine whether changes in plasma insulin levels could translate into altered CNS insulin

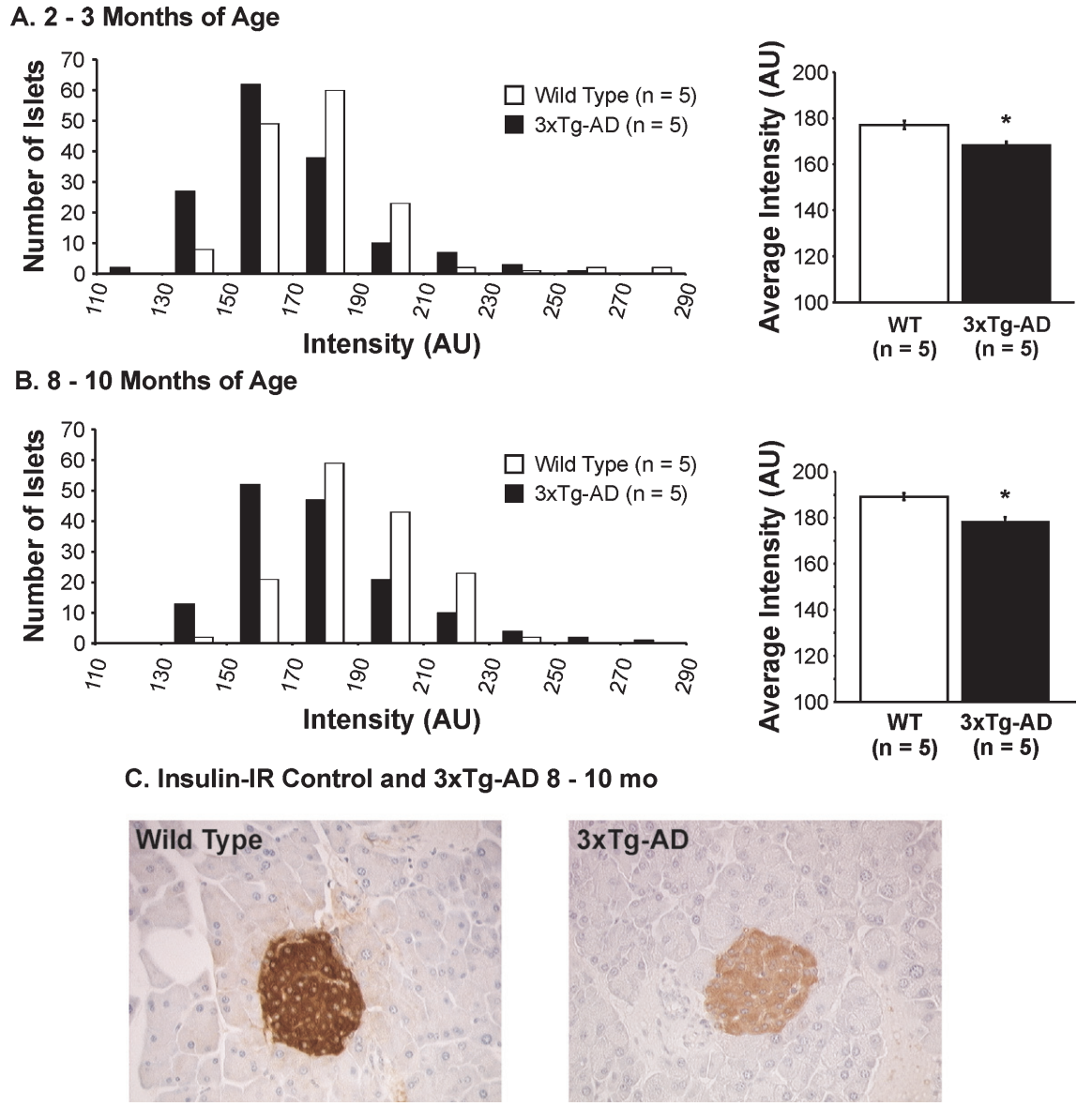

Fig. 6. Insulin immunoreactivity in pancreatic islet cells. The number of pancreatic islets displaying each given intensity of insulin immunoreactivity is shown in the graphs on left; the average intensity of islet insulin immunoreactivity in 3xTg-AD and control mice is shown on the right. Evaluation of the insulin immunoreactivity in 2-3-month-old (A) and 8-10-month-old (B) groups revealed a significant reduction in islet insulin immunoreactivity in 3xTg-AD compared to wild type control mice at both age groups examined; $^{*}p < 0.05$ versus control. C) Examples of insulin-immunoreactivity in 8-10-month-old wild type control (left) and 3xTg-AD mice (right). Note the decreased insulin immunoreactivity in the 3xTg-AD pancreas.

signaling, we first examined the MAPK/ERK pathway by western blotting. Total and phosphorylated levels of MAPK/ERK p42 and p44 (threonine 202 and tyrosine 204, respectively) were measured in the hippocampus of 3xTg-AD mice at 6-8 months and 18–20 months of age. As shown in Fig. 7, no significant change in basal or phosphorylated (activated) MAPK/ERK subunits was observed in either group of 3xTg-AD mice compared to controls (Fig. 7; 18–20-month-old group, pMAPK/ERK $p = 0.14$). These data suggest that the MAPK/ERK signaling pathway is not altered in 3xTg-AD mice.

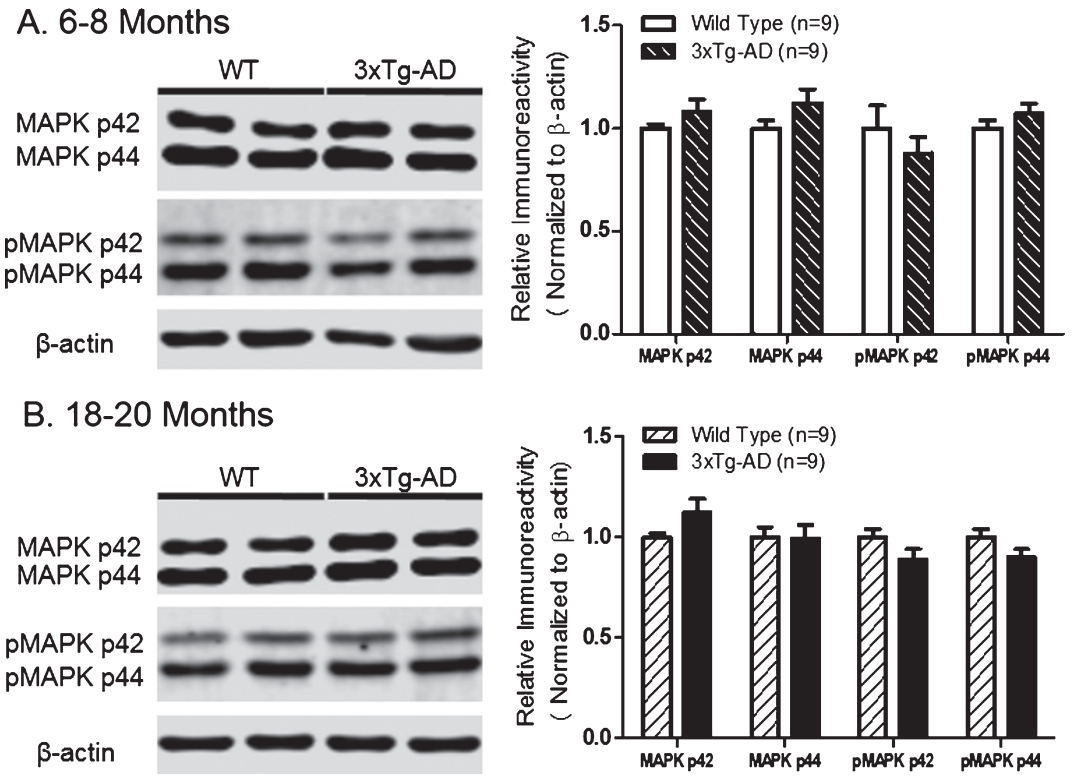

Fig. 7. MAPK/ERK signaling in the 3xTg-AD mouse hippocampus was not altered compared to wild type mice. A) Representative immunoblot (left) and normalized densitometric quantification of MAPK p42 and p44 and their phosphorylation states at Thr202 and Tyr204 (right) from 6-8-month-old wild type and 3xTg-AD mice. B) Representative immunoblot (left) and normalized densitometric quantification of MAPK p42 and p44 and their phosphorylation at Thr202 and Tyr204 (right) in 18-20-month-old wild type and 3xTg-AD mice. No significance differences in any of the components of the MAPK/ERK pathway was found between wild type and 3xTg-AD mice in either age group.

IRS1 and AKT phosphorylation is decreased in the hippocampus of old, but not young, 3xTg-AD mice

We also examined the PI3K/AKT insulin signaling pathway in the hippocampus of 3xTg-AD and wild type control mice (6-8, 16-18, and 18–20 months old) using western blots to assess IRS-1, phosphorylated IRS-1 (ser307), AKT and phosphorylated AKT (ser473). No significant changes were detected in the basal levels of IRS-1 or AKT in any age group. In contrast, we saw a significant decrease in phosphorylated IRS-1 and phosphorylated AKT in 18-20-month-old 3xTg-AD mice (Fig. 8C; pIRS-1, $p = 0.02$; pAKT, $p < 0.0001$); a difference not observed in younger transgenic mice. This suggests that insulin signaling through PI3K/AKT is likely to be somehow altered in aged 3xTg-AD mice. The appearance of decreased IRS1 and AKT phosphorylation appears to correlate with the detection of cognitive impairment in 3xTg-AD mice, but occurs well after the appearance of the classical neuropathological hallmarks of AD.

Decreased pGSK3 and increased p-Tau in the hippocampus of 3xTg-AD mice

To begin to examine downstream changes associated with altered PI3K/AKT signaling, western blots were used to assess GSK3α and β and their phosphorylation at ser21 and 9, respectively, in the hippocampus of 6-8, 16-18, and 18-20-month-old 3xTg-AD and control mice. No changes were seen in either basal or phosphorylated levels in 3xTg-AD mice compared to wild type controls at either 6-8 months (Fig. 9A) or 16-18 months (Fig. 9B) of age. Basal levels of GSK3α or GSK3β, or phosphorylated GSK3α, were also not altered in 18-20-month-old 3xTg-AD mice (Fig. 9C). However, a significant decrease in the phosphorylation of GSK3β was observed (Fig. 9C; $p = 0.001$).

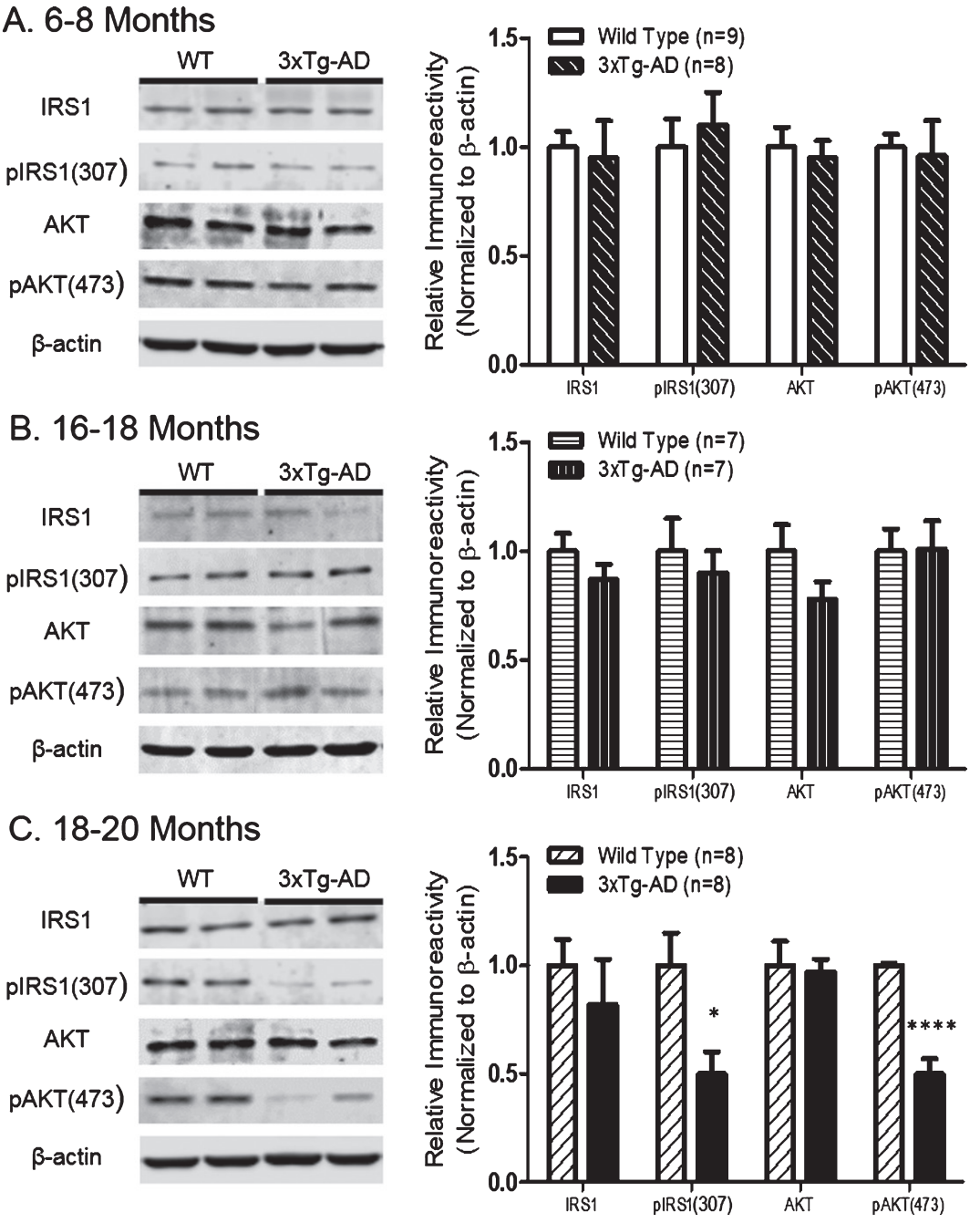

Fig. 8. PI3K/AKT signaling was significantly decreased in the hippocampus only in 18-20-month-old 3xTg-AD compared to wild type mice. A) Representative immunoblot (left) and normalized densitometric quantification (right) of IRS-1, pIRS-1 (ser307), AKT and pAKT (ser473) in the hippocampus of 6-8-month-old wild type and 3xTg-AD mice. B) Representative immunoblot (left) and normalized densitometric quantification (right) of IRS-1, pIRS-1 (ser307), AKT, and pAKT (ser473) in the hippocampus of 16-18-month-old wild type and 3xTg-AD mice. C) Representative immunoblot (left) and normalized densitometric quantification (right) of IRS-1, pIRS-1 (ser307), AKT, and pAKT (ser473) in the hippocampus of 18-20-month-old wild type and 3xTg-AD mice. No significant change in total or phosphorylated levels of IRS-1 and AKT were observed in 6-8- or 16-18-month-old 3xTg-AD mice compared to controls, but in 18-20-month-old 3xTg-AD mice, there was a significant decrease in the phosphorylation of both IRS-1 and AKT, although total IRS-1 and AKT levels were not different. $^{*}p < 0.05$, $^{****}p < 0.0001$.

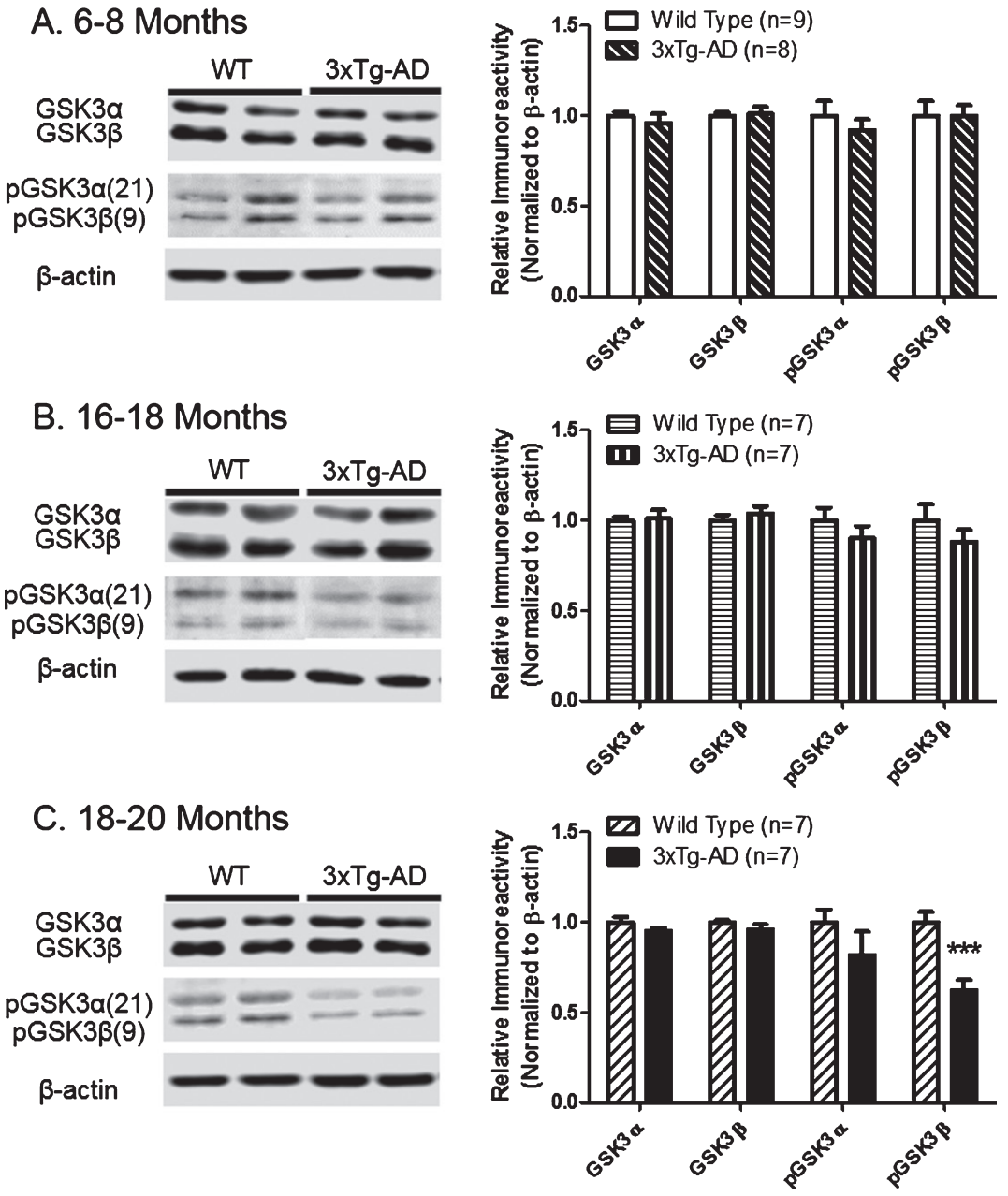

Fig. 9. pGSK3β was decreased in the hippocampus of 18-20-month-old 3xTg-AD mice. Representative immunoblot and normalized densitometric quantification of GSK3α, GSK3β, pGSK3α (Ser21), and pGSK3β (Ser9) in the hippocampus of 6-8-month-old (A), 16-18-month-old (B), and 18-20-month-old (C) 3xTg-AD mice compared to wild type controls. These experiments revealed no significant difference in GSK3α/β or pGSK3α/β in the hippocampus of younger 3xTg-AD mice compared to controls. In contrast, in the hippocampus of 18-20-month-old 3xTg-AD mice, there was a significant decrease in pGSK3β but no change in GSK3α/β or pGSK3α. $^{***}p < 0.001$.

This decrease in pGSK3β in 3xTg-AD mice was only seen at an age in which pAKT was also decreased. This suggests that decreased pGSK3β is a consequence of decreased AKT phosphorylation, since AKT is known to phosphorylate GSK3. Because GSK3 regulates tau phosphorylation, we examined the latter using western blots and antibodies directed towards tau phosphorylation (Ser396 and Ser202/Thr205), both of which are known to contribute to the paired helical filament formation associated with neurofibrillary tangles [34]. A significant increase in tau phosphorylation was observed

in 3xTg-AD mice compared to wild type controls at all ages examined [6-8 month old mice: pTau (Ser396), $p = 0.03$; pTau (Ser202/Thr205), $p < 0.001$; 16-18 month old mice: pTau (Ser396), $p = 0.04$; pTau (Ser202/Thr205), $p < 0.001$); 18-20 month mice: pTau (Ser396), $p = 0.03$; pTau (Ser202/Thr205), $p < 0.001$]. These data are shown in Fig. 10, right. When all age groups were considered, increases in pTau did not parallel the changes in GSK3β phosphorylation. However, while increased hippocampal pTau was detectable well before the appearance of spatial learning and memory impairments and changes in GSK3β phosphorylation, it is interesting to note that by 18 months of age immunoreactivity for p-Tau was highly concentrated in the principal neurons of the subiculum and CA1 (Fig. 1O).

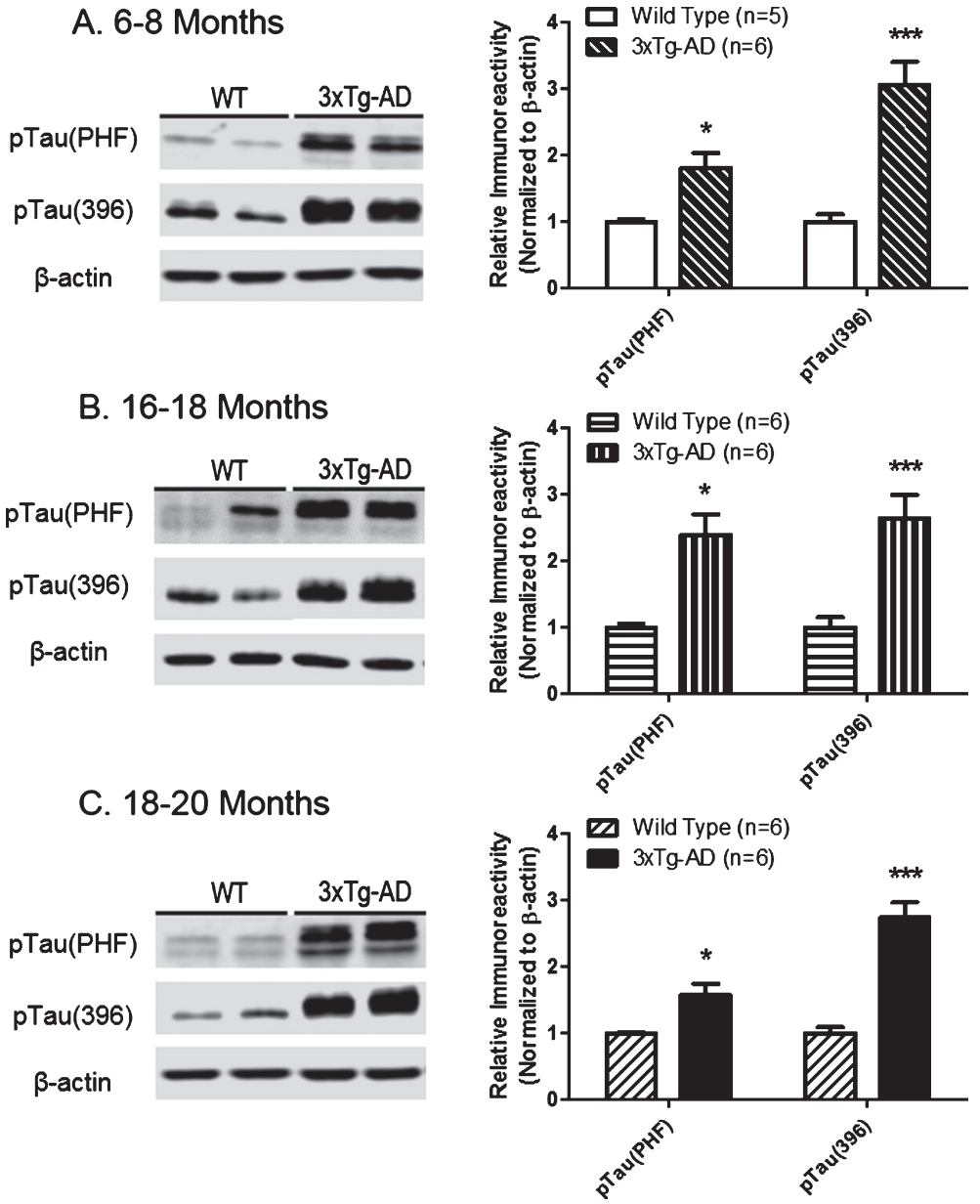

Fig. 10. pTau was significantly elevated in 3xTg-AD compared to wild type mice at all ages examined. Representative immunoblot and normalized densitometric quantification of pTau (Ser396) and pTau (Ser202/Thr205; PHF) in the hippocampus of 6-8-month-old (A), 16-18-month-old (B), and 18-20-month-old (C) 3xTg-AD mice compared to wild type controls. These experiments revealed that pTau (Ser 396) and pTau (Ser 202/Thr205; PHF) were significantly increased in the hippocampus of all age groups of 3xTg-AD mice. $^{*}p < 0.05$, $^{***}p < 0.001$.

Decreased plasma membrane GLUT3 in the hippocampus of Old 3xTg-AD mice

Insulin has recently been shown to regulate the translocation of glucose transporters into neuronal membranes in a PI3K/AKT-dependent manner. Consequently, we also examined whether the decrease in PI3K/AKT activation seen in aged 3xTg-AD mice resulted in a decrease in glucose transporter translocation. Plasma membrane and total levels of GLUT3 and GLUT4 were examined in 6-8, 16-18, and 18-20-month-old 3xTg-AD and wild type control mice using western blotting (Fig. 11). Total levels of GLUT3 or GLUT4 were not significantly altered in any age group. Additionally, there were no significant changes in the plasma membrane levels of GLUT3 or GLUT4 in the two younger age groups, or in GLUT4 plasma membrane levels in the 18-20-month-old transgenic mice. However, there was a significant reduction in plasma membrane GLUT3 (Fig. 11C; $p < 0.0001$) in 18-20-month-old 3xTg-AD mice compared to controls, suggesting that translocation of GLUT3 was decreased. Since this change was observed only in the oldest age group and correlated with alterations in the PI3K/AKT signaling pathway, it is plausible that this decrease in GLUT3 translocation is a consequence of decreased AKT phosphorylation and likely an alteration in insulin signaling.

DISCUSSION

Emerging clinical data reveal a strong link between impaired peripheral glucose regulation, insulin signaling/sensitivity and aging/AD. These data include: 1) diabetes dramatically increases the risk of cognitive decline and dementia, especially AD [1–6, 35, 36]; 2) AD patients often exhibit altered peripheral glucose regulation, characterized by either hyperinsulinemia and insulin resistance [18, 36–39], hypoinsulinemia [18], or impaired insulin secretion [19]; 3) alterations in insulin signaling are seen in postmortem AD brain tissue [40–45]; and 4) insulin acts as a cognitive enhancer in healthy aged individuals and AD patients with mild to moderate cognitive decline [46]. Further, AD mouse models have recently been shown to exhibit impaired peripheral glucose tolerance when presented with a glucose challenge [21–26]. However, findings from animal model studies have been inconsistent, possibly due to differences in background strain used (the same model can exist on different backgrounds) and/or the stage of estrus of female rodents when they are used; both factors are known to affect peripheral metabolic phenotype [47–50]. In the current study, male 3xTg-AD mice on a C57BL/6J-129S1/SvlmJ background were used to examine the relationship of peripheral metabolic phenotype to the development of AD-pathology and cognitive impairment. Further, we sought to assess whether there was an association between impaired peripheral metabolism (i.e. altered insulin levels/signaling) and the two primary hippocampal insulin signaling pathways (i.e., MAPK/ERK and PI3K/AKT). We hypothesized that hippocampal insulin signaling would be altered in 3xTg-AD mice subsequent to altered peripheral insulin levels/sensitivity since the periphery is the primary source of CNS insulin [51].

The main findings from the current study were: 1) peripheral glucose tolerance was impaired as early as 1–3 months in 3xTg-AD mice, a time point prior to the detection of neuropathological or cognitive changes; 2) impaired glucose tolerance in 3xTg-AD mice was associated with a decrease in fasting plasma insulin levels and insulin secretion following a glucose bolus, but peripheral insulin sensitivity did not appear to be altered; 3) the decrease in fasting plasma insulin and insulin secretion correlated with a decrease in insulin immunoreactivity in pancreatic islets in 3xTg-AD mice; 4) phosphorylation (activation sites) of the PI3K/AKT, but not MAPK/ERK signaling pathway, was decreased in 3xTg-AD mice concurrent with the detection of cognitive impairment; 5) the downstream target of PI3K/AKT, pGSK3β, was decreased in cognitively impaired 18-20-month-old 3xTg-AD mice; and 6) hippocampal GLUT3, but not GLUT4, translocation was decreased in 18-20-month-old 3xTg-AD mice, but not at earlier time points, and coincided with the decrease in AKT phosphorylation.

Thus, 3xTg-AD mice exhibit impaired peripheral glucose regulation early in life. However, alterations in one of the two primary insulin signaling pathways was not seen until much later (18–20 months of age) when cognitive impairment was present. These data raise the possibility that decreased AKT phosphorylation and altered CNS insulin signaling could contribute to AD-related cognitive decline. These alterations may potentially be independent of peripheral insulin levels, or may require a long-term compromise in peripheral metabolic phenotype coupled with the presence of other factors associated with AD pathogenesis (e.g., increased Aβ levels).

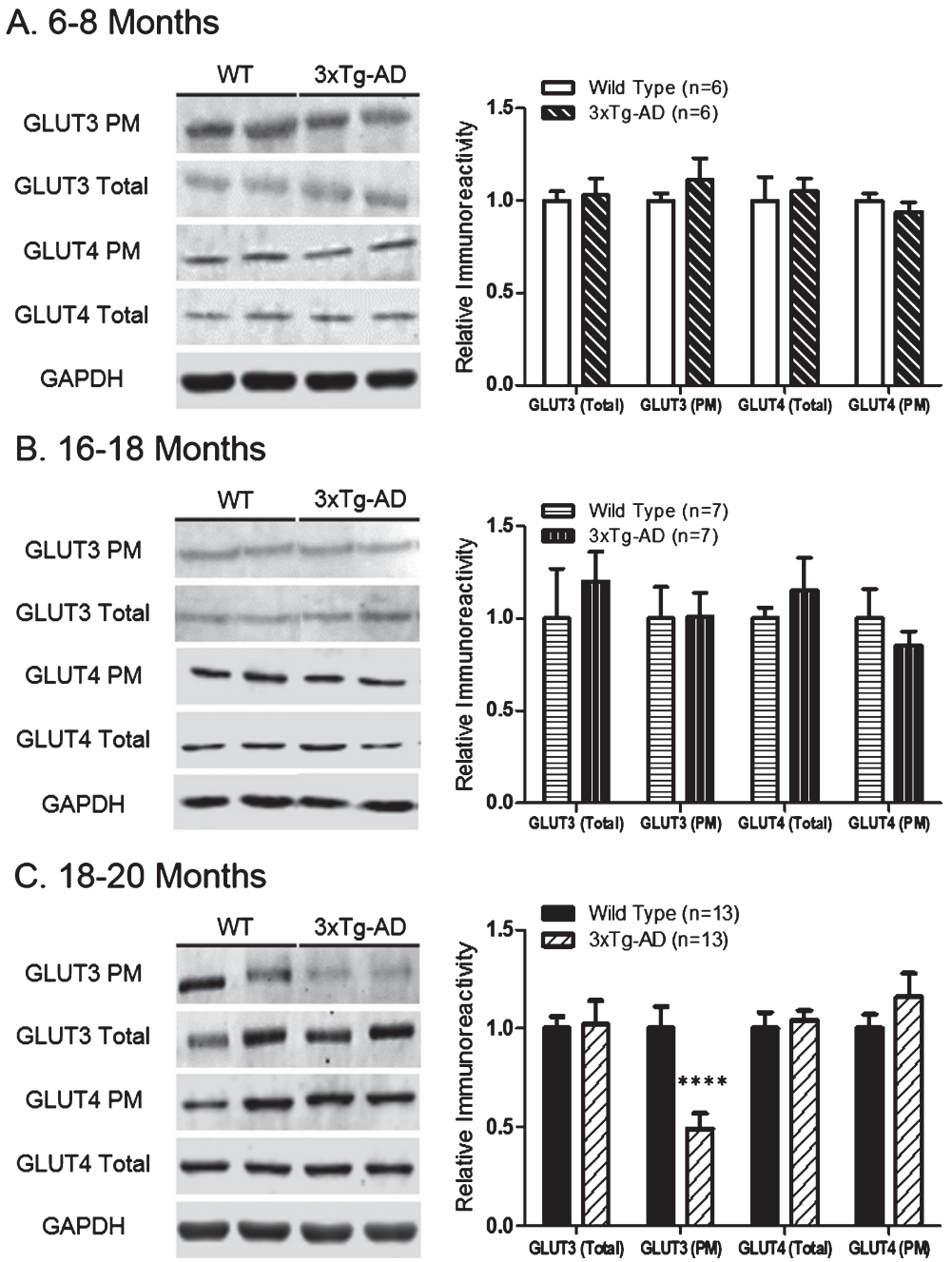

Fig. 11. Translocation of GLUT3 was significantly reduced in 18-20-month-old 3xTg-AD mice. Representative immunoblot and normalized densitometric quantification from 6-8-month-old (A), 16-18-month-old (B), and 18-20-month-old wild type and 3xTg-AD mice are shown. Total levels of hippocampal GLUT3 and GLUT4 were not different at any age. Further, no significant differences were noted in plasma membrane levels of GLUT4 in 6-8, 16-18, or 18-20-month-old 3xTg-AD hippocampus, or in plasma membrane levels of GLUT3 in 6-8 or 16-18-month-old 3xTg-AD hippocampi, compared to controls. In contrast, a significant reduction in plasma membrane GLUT3 was observed in 18-20-month-old 3xTg-AD hippocampi, suggesting that translocation of GLUT3 is decreased in 3xTg-AD mice at this later age. $^{****}p < 0.0001$.

Neuropathology and cognitive decline

Published reports indicate that the age at which AD-like changes in brain morphology and function occurs in 3xTg-AD mice varies between laboratories, presumably due to differences in background strain, housing, diet, and/or penetrance in mice when a mixed background is used. Thus, we first needed to establish the time course of Aβ deposition, tau hyperphosphorylation, and cognitive decline in our colony. While Oddo et al. [27] originally reported that extracellular Aβ-containing plaques were present as early as 6 months of age, and that by 12 months neurofibrillary tangles appeared, we did not see plaque formation until 14 months of age and a dramatic increase in hyperphosphorylated tau in principal neurons until 18 months of age. Our results are consistent with other recent studies reporting Aβ plaque formation at around 12–15 months and neurofibrillary tangles at 18 months [31, 52]. While some groups have reported cognitive changes as early as 4 months of age [53], we did not observe consistent decline in Morris water maze performance until much later: an altered learning curve was noted at 14–16 months and impaired learning and memory was seen in 3xTg-AD mice $\geq$18 months of age.

It is important to note that the mechanisms underlying AD-related cognitive decline are still unclear. For example, while numerous investigators have suggested that Aβ (plaques and, more recently, oligomers) and/or tau phosphorylation/tangle formation are responsible for AD-related cognitive decline, emerging data from clinical trials suggest that this may not be entirely so. To date, no late stage (phase III) clinical trials targeting Aβ [54–56] or tau [57, 58] have been successful. Further, clinical data reveal that subjects can exhibit AD-related neuropathology (plaques and tangles) yet remain cognitively intact and, conversely, that subjects can exhibit AD-related dementia yet have little to no neuropathology [59–64]. These confounding observations have led to the propositions that: 1) a more detailed description of the biological and cognitive characteristics of AD is required; and 2) that other factors such as vascular changes, metabolic changes, neuroinflammation, cholinergic loss, or neuronal/synapse loss may also contribute to AD-related cognitive decline and thus co-therapeutic approaches are needed. Our study suggests a novel mechanism that could also contribute to AD-related cognitive decline, namely a decrease in glucose transporter translocation due to compromised insulin signaling (see below).

Glucose tolerance

Our experiments revealed that glucose tolerance, as assessed with an ipGTT, was impaired beginning as early as 1–3 months of age in our male 3xTg-AD mice. Fasting glucose levels were elevated in 3xTg-AD mice compared to controls at 1–3 months of age, but not at later time points. These data suggest that while 3xTg-AD mice do not exhibit a "diabetic" phenotype (i.e., elevated fasting glucose), peripheral glucose dysregulation can be revealed by a metabolic challenge with an exogenous glucose bolus. It has been suggested that screening for a pre-diabetic phenotype (impaired glucose tolerance; altered insulin response) versus a true diabetic phenotype (i.e., altered fasting glucose levels) could be an important biomarker for assessing the risk for developing AD [19, 65].

It is unclear why or how peripheral metabolic alterations arise in AD mouse models. Prominent possibilities include intrinsic alterations in peripheral organs, or subpathological changes within the CNS that affect the periphery (e.g., Aβ oligomers modifying hypothalamic or brainstem function). While the brainstem is not typically assessed for plaques in murine AD models due to histological preparation of the brain for sectioning (i.e., cerebellum and brainstem are cut off), we did not see any hypothalamic Aβ plaques in our 18-month-old 3xTg-AD mice (data not shown) as was previously reported by Do et al. [66] and human studies suggest that Aβ pathology within these brain regions only occurs at much later stages of AD pathogenesis [67]. Regardless, data suggest that peripheral metabolic alterations and AD-related pathogenesis are likely to affect each other, thereby creating a dangerous feedback loop. For example, pre-diabetic alterations such as hyperglycemia can affect Aβ production. Indeed, acute hyperglycemia raises interstitial fluid Aβ levels [68] and experimentally induced diabetes increases Aβ plaque load in AD mouse models [13, 69]. In turn, Aβ can have neurotoxic effects [70], inhibit synaptic plasticity/signaling [71, 72], and can negatively affect insulin signaling by decreasing insulin receptor density/number on dendritic spines [73].

Plasma insulin

A compromise in glucose tolerance could occur due to either a decrease in peripheral insulin levels, a decrease in insulin receptor sensitivity due to hyperinsulinemia, or as a secondary consequence

of obesity and increased food intake. While no difference in body weight or food intake was seen in 3xTg-AD mice, compared to controls, significant decreases in fasting plasma insulin levels and 15 min following a glucose bolus were seen in 3xTg-AD mice as early as 1–3 months of age and persisted throughout their life. No difference in insulin sensitivity was observed between groups at any time point examined. Thus, reduced insulin levels, and not a decrease in insulin receptor sensitivity, are likely to contribute to the disrupted glucose tolerance in 3xTg-AD mice. It is interesting to note that one of the largest population-based longitudinal studies suggests that decreased insulin following an oral glucose challenge, not insulin receptor sensitivity, poses the greater risk for developing AD [19]. Nekrep et al. [74] reported that neural crest derived cells are present in the pancreas and contribute to pancreatic beta cell development and insulin production and/or secretion. Given the common ancestry of neural crest cells and neuroectoderm, it is possible that Thy1.2-regulated genes are expressed in both cell populations and subsequently could underlie the reduced pancreatic insulin staining we observed in 3xTg-AD mice. Due to technical problems we were unable to determine whether Aβ or plaques were present in the pancreas of our 3xTg-AD mice. However, Vandal et al. [24] reported that human AβPP was found in the 3xTg-AD pancreas. Thus, it is possible that pancreatic Aβ could have played a role in the reduced insulin production we observed in the 3xTg-AD mice, although definitive studies are necessary. Further, this result does not rule out the possibility that other metabolic alterations (e.g., potential alterations in glucagon, leptin, GLP1) could also be contributing to the impairment in peripheral glucose tolerance in 3xTg-AD mice.

Hippocampal insulin signaling in 3xTg-AD mice

Changes in peripheral insulin levels are likely to affect CNS insulin signaling. Insulin, among other signaling molecules, stimulates the MAPK/ERK and PI3K/AKT pathways, and both pathways have been linked with learning and memory [75–82]. In our study, no differences in the MAPK/ERK signaling pathway were observed in 3xTg-AD mice at either 6-8 or 18-20 months of age. While this was somewhat surprising given the lifelong change in peripheral insulin levels, MAPKs are also activated when exposed to an inflammatory environment. The MAPKs are composed of a family of related serine/threonine protein kinases, such as JNK, ERK, and p38 MAPK, which can be activated in response to cellular stimuli such as stress, inflammatory cytokines (e.g., tumor necrosis factor (TNF)-α and interleukin (IL)-1β), or G protein coupled receptor agonists [83, 84]. 3xTg-AD mice exhibit increased inflammatory markers, including TNF and reactive astrogliosis [85–88]. Thus MAPK/ERK signaling could be maintained due to increased oxidative stress even if plasma and CNS insulin levels were reduced. Additionally, while some studies have shown that Aβ can inhibit ERK1/2 [89], others have suggested that Aβ has no effect on MAPK signaling [90] or can even increase ERK1/2 activity [91]. Thus, despite data linking MAPK/ERK with cognitive function, it is unlikely that a disruption of this pathway played a primary role in the impairments we observed in our 3xTg-AD mice.

PI3K/AKT pathway activity has been shown to be reduced in human AD brain tissue [42, 44], and recent studies suggests that alterations in this pathway can also be seen in 3xTg-AD mice [25, 92]. Our results demonstrated no significant difference in the PI3K/AKT insulin signaling pathway at 6-8 and 16-18 months of age, but at 18–20 months there was a significant reduction in the phosphorylation of AKT at serine 473 and IRS-1 at serine 307. AKT is considered to be the primary regulator of insulin's metabolic effects. Our current results are in contrast to a previously published study suggesting that altered insulin signaling occurred prior to a change in glucose tolerance. Specifically, Velazquez and colleagues [25] showed a decrease in IRS-1 and the phosphorylation of IRS-1 at ser612 at 10 months of age, although no change in the GTT was seen until later. Further, they reported an increase in phosphorylation of AKT at both serine 308 and 473 at 16 months of age when impaired glucose tolerance was observed. The reason for the difference with our current study is unclear, but could be the result of gender differences (female versus male mice). Additionally, their study used a cortex-hippocampus homogenate, while ours was solely hippocampus, potentially producing a dilution effect since not all cortical regions are uniformly affected in AD.

In the presence of insulin, IRS1 becomes phosphorylated at tyrosine residues to cause its activation, while IRS1 serine phosphorylation inhibits its activity. Serine phosphorylation is increased by inflammasomes such as TNF and has been suggested to be linked to insulin resistance [93–95]. Indeed, several studies have reported increased serine phosphorylation of IRS1 in human AD tissue and mouse

models [40, 45, 96]. Thus, in our current study it is surprising to see a decrease in IRS1 serine phosphorylation based on previous studies and the reported increase in neuroinflammation in old 3xTg-AD mice [85–87]. However, IRS1 serine 307 phosphorylation has also been shown to occur via AKT in a negative feedback mechanism. Specifically, an increase in insulin induced serine 307 phosphorylation of IRS1 can be blocked by the PI3K inhibitor LY290042 [95]. Given the observed decrease in AKT phosphorylation concomitant with the decrease in IRS1 serine 307 phosphorylation, it is clear additional research is required to truly understand the dynamics of insulin signaling under "normal" physiological conditions as well as in AD.

Following activation of IRS-1, AKT becomes phosphorylated at ser308 by PI3K and then by mTOR at serine 473 to become fully activated. We have shown that serine 473 phosphorylation is decreased, but only at the latest time point examined (18–20 months of age). While peripheral insulin levels were decreased in 3xTg-AD mice relative to wild type controls as early as 1 month of age, no change in hippocampal insulin signaling was observed until after neuropathology was detected. Although we cannot rule out the possibility that IRS1/AKT phosphorylation is altered in other brain regions prior to neuropathology, this represents a disconnect between peripheral insulin levels and hippocampal insulin signaling. This is fascinating since CNS insulin is believed to be primarily derived from the periphery through a saturable transport mechanism though several lines of evidence suggest that it is also produced in the CNS [97, 98]. What could underlie this disconnect? Aβ has been shown to reduce responsiveness to insulin in presynaptic terminals [92, 99] and ADDLs can cause a loss of neuronal surface IRs [70]. Thus, a parsimonious explanation for the delayed reduction in CNS insulin signaling in 3xTg-AD mice is that a combination of factors may be required to produce this result. Specifically, it is possible that a decreased supply of peripheral insulin, coupled with an increased Aβ production, may be required to perturb hippocampal insulin signaling. In addition, insulin and IGF1 have similar structures and can bind both receptors, thus it is possible that a change in IGF1 could result in altered insulin signaling. Indeed, it has been shown that IGF1 receptor is decreased in 3xTg-AD mice [92]. However, they saw no change in the phosphorylation of IGF1 and since insulin has a much higher affinity for insulin receptor it is more likely that insulin is responsible for the decrease in phosphorylation of downstream targets. Another factor that could be leading to altered PI3K/AKT signaling is inflammation induced from Aβ production and tau hyperphosphorylation. 3xTg-AD mice have been shown to have increased levels of inflammatory markers [85–87] and inflammatory mediators such as TNF, JNK, IKK, and protein kinase C (PKC), which can inhibit insulin action by serine phosphorylation of IRS1. Further, serine/threonine kinases involved in insulin signaling can also be directly activated by reactive oxygen species, and increased reactive oxygen species levels are one of the major co-pathologies in aging and AD [100, 101]. Since this study did not examine inflammation in 3xTg-AD mice, or all phosphorylation sites of IR and IRS1, it is possible that increased inflammation leads to increased inhibitory phosphorylation of these proteins and to decreased PI3K/AKT signaling. Conversely, PI3K/AKT signaling has also been shown to play a major role in inducing inflammation (for review, see [102]) and it has been shown that inhibition of the PI3K/AKT signaling pathway can enhance the activation of inflammatory mediators [103, 104].

Interestingly, the change in PI3K/AKT signaling occurred only at a time point when a decline in cognitive function was present. In some initial studies, intranasal insulin has been shown to improve cognition in patients with mild-moderate AD, patients with mild cognitive impairment, as well as in normal patients [46, 104, 105]. Further, insulin has also been shown to improve spatial memory in 3xTg-AD mice along with increasing AKT activation [98]. Taken together, these results suggest that decreased AKT phosphorylation could contribute to the cognitive decline in 3xTg-AD mice and humans with AD, especially given the apparent role of insulin-AKT signaling in normal cognitive function [73–78], and that supplying insulin directly to the brain via intranasal delivery could help relieve cognitive dysfunction by restoring insulin signaling via the PI3K/AKT pathway.

pGSK3β is decreased in old 3xTg-AD mice

Glycogen synthase kinase-3 (GSK3α/β) is a constitutively active, ubiquitous serine/threonine kinase [106], that is critical for neuronal function [107–109]; overexpression has been linked with cell death [110–114] and a reduction in cell proliferation [115, 116]. Since we have shown that AKT phosphory-

lation (activation) is decreased in 18-20-month-old 3xTg-AD mice, and since GSK3 inhibition is primarily mediated by PI3K/AKT via serine phosphorylation [110], we also examined GSK3 levels and its phosphorylation. Levels of GSK3 were not altered in 3xTg-AD mice. However, phosphorylation of GSK3β at serine 9 is decreased in 3xTg-AD mice at 18–20 months of age, but not at earlier time points, suggesting that this is likely to occur subsequent to the decrease in pAKT. This decrease in GSK3β phosphorylation could lead to GSK3 hyperactivation, increasing Aβ production and toxicity [117–120] neuroinflammation [121, 122] and tau phosphorylation [123, 124]. Thus, a decrease in GSK3 phosphorylation could further contribute to AD neuropathogenesis and cognitive decline.

Tau phosphorylation occurring prior to the change in pGSK3β seems paradoxical, but is likely because the human transgene expressed in 3xTg-AD mice produces a mutated version of tau that is highly susceptible to phosphorylation. What is interesting, however, is that the apparent increase in tau hyperphosphorylation and eventual deposition in principal neurons (i.e., 18 months; Fig. 1O) only occurred around the same time as the observed decrease in AKT phosphorylation and GSK3β inhibition. Further experiments are needed to directly test whether this is a cause and effect relationship.

Reduced GLUT3, but not GLUT4, translocation in the hippocampus of old 3xTg-AD mice

Insulin's effects on learning and memory have been suggested to be largely independent of glucose utilization. Whether this assertion is valid is unclear, since recent studies have shown that: 1) insulin can stimulate neural glucose uptake in medial temporal lobe structures involved in learning and memory [125, 126]; 2) subjects with insulin resistance exhibit a regional reduction in glucose metabolism [16] that can be improved with exogenous insulin administration [21]; 3) conditional insulin receptor knock out mice (NIRKO) exhibit decreased glucose uptake in their brain [127]; 4) the expression or translocation of several of the facilitated glucose transporters (i.e., GLUT1, GLUT3, and GLUT4) can be affected by insulin/IGF1 signaling or insulin sensitizing drugs [128, 129]; and 5) studies have shown that a subject's performance on hippocampal-dependent cognitive tasks is dependent on glucose uptake and that increasing the hippocampal glucose supply can enhance memory performance [130–132]. Taken together, these studies suggest that insulin affects neuronal/network glucose utilization and, subsequently, learning and memory.

Recent data demonstrate that translocation of the primary neuronal glucose transporter, GLUT3, to the plasma membrane is insulin dependent and involves the PI3K/AKT pathway, although neuronal depolarization is also required [129]. In this regard, metabolically challenging the hippocampus (e.g., during a cognitive task) should lead to GLUT3 translocation to allow for the increased demand for glucose. Interestingly, GLUT3 protein levels are decreased in post-mortem tissue from AD patients [133] and in patients with type 2 diabetes [134]. Aβ can also decrease glucose uptake by inhibiting GLUT3 fusion with the membrane, suggesting that a decrease in translocation, rather than GLUT3 expression, is critical for overall GLUT3 function [135]. We found that decreased GLUT3 translocation correlated with reduced AKT phosphorylation, suggesting that this may be a downstream effect of altered CNS insulin signaling in 3xTg-AD mice. Further, the decrease in GLUT3 translocation corresponded with the first detection of cognitive impairment. This timing could reflect a potential cause and effect relationship between decreased GLUT3 translocation and cognitive decline.

The majority of glucose uptake in peripheral tissues is under the control of insulin via the insulin-sensitive glucose transporter, GLUT4 [136]. Recently it has been suggested that a similar mechanism may occur in the hippocampus since GLUT4 is found there [137–139] and the hippocampus also contains high levels of the insulin receptor [140–143]. Indeed, it has now been shown that GLUT4 translocation is insulin sensitive in the hippocampus and is also PI3K/AKT dependent [128, 144]. Surprisingly, no change in GLUT4 translocation was observed in 3xTg-AD mice in this study despite the decrease in AKT phosphorylation. However, several factors other than insulin can affect GLUT4 translocation including PKC, tumor necrosis factor-α, AMP kinase, endothelin and leptin [144–149]. Additionally, chronic exposure to either leptin or insulin has been shown to decrease GLUT4 at the mRNA and protein levels [144]. Further, insulin may increase GLUT4 translocation in an activity-dependent manner. Thus, a number of simultaneously acting factors could have contributed to the lack of change we observed in GLUT4 translocation in our 3xTg-AD mice.

Summary

In summary, our study provides evidence that impaired peripheral glucose tolerance, likely the consequence of low insulin levels, is present in 3xTg-AD mice prior to any neuropathological changes or cognitive decline. Interestingly, despite low peripheral insulin levels early on, 3xTg-AD mice did not exhibit alterations in the insulin AKT pathway (i.e., decreased phosphorylation) until later time points when cognitive decline was first detected. Therefore, AD-related alterations in CNS insulin signaling is not likely to be simply a reflection of peripheral insulin levels but may require an interaction between these peripheral changes and changes associated with AD pathogenesis (i.e., increased Aβ production). Further, the decrease in serine phosphorylation of IRS1 concomitant with a decrease in AKT phosphorylation suggests that changes in insulin signaling pathways are likely to be more complex in AD and that additional factors are involved. Regardless, a decrease in GLUT3 translocation may be the direct result of altered insulin signaling. This decrease in GLUT3 at the cellular membrane could result in impaired neuronal glucose uptake, thereby depriving neurons of sufficient glucose during a time of increased metabolic demand (i.e., during the performance of cognitive tasks) and could contribute to the hypometabolic phenotype seen in AD, providing a potential mechanism whereby intranasal insulin exerts its beneficial effects. Finally, the observation that several AD mouse models exhibit a pre-diabetic phenotype (i.e., impaired glucose tolerance) months prior to being able to detect any neuropathology or cognitive decline raises the possibility that this could be a beneficial biomarker for detecting subjects with an increased risk for developing AD.

ACKNOWLEDGMENTS

This research was funded through the support of the Illinois Department of Public Health (PRP), Center for Alzheimer's Disease and Related Disorders CADRD: SIU-SOM; PRP) and Center for Integrated Research in Cognitive and Neural Sciences (GMR; PRP).

Authors' disclosures available online (https://www.j-alz.com/manuscript-disclosures/18-0707r2).

REFERENCES

[1] Arvanitakis Z, Wilson RS, Bienias JL, Evans DA, Bennett DA (2004) Diabetes mellitus and risk of Alzheimer disease and decline in cognitive function. *Arch Neurol* **61**, 661.

[2] Leibson CL, Rocca WA, Hanson VA, Cha R, Kokmen E, O'Brien PC, Palumbo PJ (1997) Risk of dementia among persons with diabetes mellitus: A population-based cohort study. *Am J Epidemiol* **145**, 301-308.

[3] Ott A, Stolk RP, van Harskamp F, Pols HA, Hofman A, Breteler MM (1999) Diabetes mellitus and the risk of dementia: The Rotterdam Study. *Neurology* **53**, 1937-1942.

[4] Sima AAF, Kamiya H, Li ZG (2004) Corrigendum to insulin, C-peptide, hyperglycemia, and central nervous system complications in diabetes. *Eur J Pharmacol* **490**, 187-197.

[5] Yaffe K, Blackwell T, Kanaya AM, Davidowitz N, Barrett-Connor E, Krueger K (2004) Diabetes, impaired fasting glucose, and development of cognitive impairment in older women. *Neurology* **63**, 658-663.

[6] Yoshitake T, Kiyohara Y, Kato I, Ohmura T, Iwamoto H, Nakayama K, Ohmori S, Nomiyama K, Kawano H, Ueda K, Sueishi K, Tsuneyoshi M, Fujishima M (1995) Incidence and risk factors of vascular dementia and Alzheimer's disease in a defined elderly Japanese population: The Hisayama Study. *Neurology* **45**, 1161-1168.

[7] Jolivalt CG, Hurford R, Lee CA, Dumaop W, Rockenstein E, Masliah E (2010) Type 1 diabetes exaggerates features of Alzheimer's disease in APP transgenic mice. *Exp Neurol* **223**, 422-431.

[8] Kim B, Backus C, Oh S, Hayes JM, Feldman EL (2009) increased tau phosphorylation and cleavage in mouse models of type 1 and type 2 diabetes. *Endocrinology* **150**, 5294-5301.

[9] Li Z, Zhang W, Sima AAF (2007) Alzheimer-like changes in rat models of spontaneous diabetes. *Diabetes* **56**, 1817-1824.

[10] Planel E, Tatebayashi Y, Miyasaka T, Liu L, Wang L, Herman M, Yu WH, Luchsinger JA, Wadzinski B, Duff KE, Takashima A (2007) Insulin dysfunction induces in vivo tau hyperphosphorylation through distinct mechanisms. *J Neurosci* **27**, 13635-13648.

[11] Cao D, Lu H, Lewis TL, Li L (2007) Intake of sucrose-sweetened water induces insulin resistance and exacerbates memory deficits and amyloidosis in a transgenic mouse model of Alzheimer disease. *J Biol Chem* **282**, 36275-36282.

[12] Clodfelder-Miller BJ, Zmijewska AA, Johnson GVW, Jope RS (2006) Tau is hyperphosphorylated at multiple sites in mouse brain in vivo after streptozotocin-induced insulin deficiency. *Diabetes* **55**, 3320-3325.

[13] Hayashi-Park E, Ozment BN, Griffith CM, Zhang H, Patrylo PR, Rose GM (2017) Experimentally induced diabetes worsens neuropathology, but not learning and memory, in middle aged 3xTg mice. *Behav Brain Res* **322**, 280-287.

[14] Ho L, Qin W, Pompl PN, Xiang Z, Wang J, Zhao Z, Peng Y, Cambareri G, Rocher A, Mobbs CV, Hof PR, Pasinetti GM (2004) Diet-induced insulin resistance promotes amyloidosis in a transgenic mouse model of Alzheimer's disease. *FASEB J* **18**, 902-904.

[15] Julien C, Tremblay C, Phivilay A, Berthiaume L, Émond V, Julien P, Calon F (2010) High-fat diet aggravates amyloid-beta and tau pathologies in the 3xTg-AD mouse model. *Neurobiol Aging* **31**, 1516-1531.

[16] Baker LD, Cross DJ, Minoshima S, Belongia D, Watson GS, Craft S (2011) Insulin resistance and Alzheimer-like reductions in regional cerebral glucose metabolism for cognitively normal adults with prediabetes or early type 2 diabetes. *Arch Neurol* **68**, 51-57.

[17] Matsuzaki T, Sasaki K, Tanizaki Y, Hata J, Fujimi K, Matsui Y, Sekita A, Suzuki SO, Kanba S, Kiyohara Y, Iwaki T (2010) Insulin resistance is associated with the pathology of Alzheimer disease: The Hisayama study. *Neurology* **75**, 764-770.

[18] Peila R, Rodriguez BL, White LR, Launer LJ (2004) Fasting insulin and incident dementia in an elderly population of Japanese-American men. *Neurology* **63**, 228-233.

[19] Rönnemaa E, Zethelius B, Sundelöf J, Sundström J, Degerman-Gunnarsson M, Berne C, Lannfelt L, Kilander L (2008) Impaired insulin secretion increases the risk of Alzheimer disease. *Neurology* **71**, 1065-1071.

[20] Van Oijen M, Okereke OI, Kang JH, Pollak MN, Hu FB, Hankinson SE, Grodstein F (2008) Fasting insulin levels and cognitive decline in older women without diabetes. *Neuroepidemiology* **30**, 174-179.

[21] Iménez-Llort L, García Y, Buccieri K, Revilla S, Suñol C, Cristofol R, Sanfeliu C (2010) Gender-specific neuroimmunoendocrine response to treadmill exercise in 3xTg-AD mice. *Int J Alzheimers Dis* **2010**, 128354.

[22] Macklin L, Griffith CM, Cai Y, Rose GM, Yan XX, Patrylo PR (2017) Glucose tolerance and insulin sensitivity are impaired in APP/PS1 transgenic mice prior to amyloid plaque pathogenesis and cognitive decline. *Exp Gerontol* **88**, 9-18.

[23] Pedrós I, Petrov D, Allgaier M, Sureda F, Barroso E, Beas-Zarate C, Auladell C, Pallàs M, Vázquez-Carrera M, Casadesús G, Folch J, Camins A (2014) Early alterations in energy metabolism in the hippocampus of APPswe/PS1dE9 mouse model of Alzheimer's disease. *Biochim Biophys Acta* **1842**, 1556-1566.

[24] Vandal M, White P, St-Amour I, Marette A, Calon F (2014) The 3xTg-AD mouse model of Alzheimer's disease exhibits age-dependent impaired glucose tolerance. *Alzheimers Dement* **10**, 305.

[25] Velazquez R, Tran A, Ishimwe E, Denner L, Dave N, Oddo S, Dineley KT (2017) Central insulin dysregulation and energy dyshomeostasis in two mouse models of Alzheimer's disease. *Neurobiol Aging* **58**, 1-13.

[26] Zhang Y, Zhou B, Zhang F, Wu J, Hu Y, Liu Y, Zhai Q (2012) Amyloid-β induces hepatic insulin resistance by activating JAK2/STAT3/SOCS-1 signaling pathway. *Diabetes* **61**, 1434-1443.

[27] Oddo S (2003) Amyloid deposition precedes tangle formation in a triple transgenic model of Alzheimer's disease. *Neurobiol Aging* **24**, 1063-1070.

[28] Griffith CM, Xie MX, Qiu WY, Sharp AA, Ma C, Pan A, Yan XX, Patrylo PR (2016) Aberrant expression of the pore-forming KATP channel subunit Kir6.2 in hippocampal reactive astrocytes in the 3xTg-AD mouse model and human Alzheimer's disease. *Neuroscience* **336,** 81-101.

[29] Reagan LP, Magariños AM, Yee DK, Swzeda LI, Van Bueren A, McCall AL, McEwen BS (2000) Oxidative stress and HNE conjugation of GLUT3 are increased in the hippocampus of diabetic rats subjected to stress. *Brain Res* **862**, 292-300.

[30] Oh KJ, Perez SE, Lagalwar S, Vana L, Binder L, Mufson EJ (2010) Staging of Alzheimer's pathology in triple transgenic mice: A light and electron microscopic analysis. *Int J Alzheimers Dis* **2010**, 780102.

[31] Mastrangelo MA, Bowers WJ (2008) Detailed immunohistochemical characterization of temporal and spatial progression of Alzheimer's disease-related pathologies in male triple-transgenic mice. *BMC Neurosci* **9**, 81.

[32] Perez SE, Lumayag S, Kovacs B, Mufson EJ, Xu S (2009) β-amyloid deposition and functional impairment in the retina of the APPswe/PS1ΔE9 transgenic mouse model of Alzheimer's disease. *Investig Opthalmology Vis Sci* **50**, 793.

[33] Grimaldi A, Brighi C, Peruzzi G, Ragozzino D, Bonanni V, Limatola C, Ruocco G, Di Angelantonio S (2018) Inflammation, neurodegeneration and protein aggregation in the retina as ocular biomarkers for Alzheimer's disease in the 3xTg-AD mouse model. *Cell Death Dis* **9**, 685.

[34] Urakami K, Mori M, Wada K, Kowa H, Takeshima T, Arai H, Sasaki H, Kanai M, Shoji M, Ikemoto K Morimatsu M (1999) A comparison of tau protein in cerebrospinal fluid between corticobasal degeneration and progressive supranuclear palsy. *Neurosci Lett* **259**, 127-129.

[35] Luchsinger JA, Reitz C, Patel B, Tang MX, Manly JJ, Mayeux R (2007) Relation of diabetes to mild cognitive impairment. *Arch Neurol* **64**, 570.

[36] Craft S, Peskind E, Schwartz MW, Schellenberg GD, Raskind M, Porte D (1998) Cerebrospinal fluid and plasma insulin levels in Alzheimer's disease: Relationship to severity of dementia and apolipoprotein E genotype. *Neurology* **50**, 164-168.

[37] Kuusisto J, Koivisto K, Mykkänen L, Helkala EL, Vanhanen M, Hänninen T, Kervinen K, Kesäniemi YA, Riekkinen PJ, Laakso M (1997) Association between features of the insulin resistance syndrome and Alzheimer's disease independently of apolipoprotein E4 phenotype: Cross sectional population based study. *BMJ* **315**, 1045-1049.

[38] Meneilly GS, Hill A (1993) Alterations in glucose metabolism in patients with Alzheimer's disease. *J Am Geriatr Soc* **41**, 710-714.

[39] Ott A, Stolk RP, Hofman A, van Harskamp F, Grobbee DE, Breteler MMB (1996) Association of diabetes mellitus and dementia: The Rotterdam Study. *Diabetologia* **39**, 1392-1397.

[40] Bomfim TR, Forny-Germano L, Sathler LB, Brito-Moreira J, Houzel JC, Decker H, Silverman MA, Kazi H, Melo HM, McClean PL, Holscher C, Arnold SE, Talbot K, Klein WL, Munoz DP, Ferreira ST, De Felice FG (2012) An anti-diabetes agent protects the mouse brain from defective insulin signaling caused by Alzheimer's disease-associated Aβ oligomers. *J Clin Invest* **122**, 1339-1353.

[41] Jolivalt CG, Lee CA, Beiswenger KK, Smith JL, Orlov M, Torrance MA, Masliah E (2008) Defective insulin signaling pathway and increased glycogen synthase kinase-3 activity in the brain of diabetic mice: Parallels with Alzheimer's disease and correction by insulin. *J Neurosci Res* **86**, 3265-3274.

[42] Liu Y, Liu F, Grundke-iqbal I, Iqbal K, Gong C (2011) Deficient brain insulin signalling pathway in Alzheimer's disease. *J Pathol* **225**, 54-62.

[43] Moloney AM, Griffin RJ, Timmons S, O'Connor R, Ravid R, O'Neill C (2010) Defects in IGF-1 receptor, insulin receptor and IRS-1/2 in Alzheimer's disease indicate possible resistance to IGF-1 and insulin signalling. *Neurobiol Aging* **31**, 224-243.

[44] Steen E, Terry BM, Rivera EJ, Cannon JL, Neely TR, Tavares R, Xu XJ, Wands JR, de la Monte SM (2005) Impaired insulin and insulin-like growth factor expression and signaling mechanisms in Alzheimer's disease–is this type 3 diabetes? *J Alzheimers Dis* **7**, 63-80.

[45] Talbot K, Wang HY, Kazi H, Han LY, Bakshi KP, Stucky A, Fuino RL, Kawaguchi KR, Samoyedny AJ, Wilson RS, Arvanitakis Z, Schneider JA, Wolf BA, Bennett DA, Trojanowski JQ, Arnold SE (2012) Demonstrated brain insulin resistance in Alzheimer's disease patients is associated with IGF-1 resistance, IRS-1 dysregulation, and cognitive decline. *J Clin Invest* **122**, 1316-1338.

[46] Craft S, Baker LD, Montine TJ, Minoshima S, Watson GS, Claxton A, Arbuckle M, Callaghan M, Tsai E, Plymate SR, Green PS, Leverenz J, Cross D, Gerton B (2012) Intranasal insulin therapy for Alzheimer disease and amnestic mild cognitive impairment: A pilot clinical trial. *Arch Neurol* **69**, 29-38.

[47] Bailey C, Matty A (2009) Glucose tolerance and plasma insulin of the rat in relation to the oestrous cycle and sex hormones. *Horm Metab Res* **4**, 266-270.

[48] Clee SM, Attie AD (2007) The genetic landscape of type 2 diabetes in mice. *Endocr Rev* **28**, 48-83.

[49] Fontaine DA, Davis DB (2015) Attention to background strain is essential for metabolic research: C57BL/6 and the International Knockout Mouse Consortium. *Diabetes* **65**, 25-33.

[50] Joost HG, Schürmann A (2014) The genetic basis of obesity-associated type 2 diabetes (diabesity) in polygenic mouse models. *Mamm Genome* **25**, 401-412.

[51] Banks WA (2004) The source of cerebral insulin. *Eur J Pharmacol* **490**, 5-12.

[52] Cai Y, Zhang XM, Macklin LN, Cai H, Luo XG, Oddo S, Laferla FM, Struble RG, Rose GM, Patrylo PR, Yan XX (2012) BACE1 elevation is involved in amyloid plaque development in the triple transgenic model of Alzheimer's disease: Differential Aβ antibody labeling of early-onset axon terminal pathology. *Neurotox Res* **21**, 160-174.

[53] Clinton LK, Billings LM, Green KN, Caccamo A, Ngo J, Oddo S, McGaugh JL, LaFerla FM (2007) Age-dependent sexual dimorphism in cognition and stress response in the 3xTg-AD mice. *Neurobiol Dis* **28**, 76-82.

[54] Ostrowitzki S, Deptula D, Thurfjell L, Barkhof F, Bohrmann B, Brooks DJ, Klunk E, Ashford E, Yoo K, Xu ZX, Loetscher H (2012) Mechanism of amyloid removal in patients with Alzheimer disease treated with gantenerumab. *Arch Neurol* **69**, 198-207.

[55] Doody RS, Thomas RG, Farlow M, Iwatsubo T, Vellas B, Joffe S, Kieburtz K, Raman R, Sun X, Aisen PS, Siemers E (2014) Phase 3 trials of solanezumab for mild-to-moderate Alzheimer's disease. *N Engl J Med* **370**, 311-321.

[56] Salloway S, Sperling R, Fox NC, Blennow K, Klunk W, Raskind M, Sabbagh M, Honig LS, Porsteinsson AP, Ferris S, Reichert M (2014) Two phase 3 trials of bapineuzumab in mild-to-moderate Alzheimer's disease. *N Engl J Med* **370**, 322-333.

[57] Gauthier S, Feldman HH, Schneider LS, Wilcock GK, Frisoni GB, Hardlund JH, Moebius HJ, Bentham P, Kook KA, Wischik DJ, Schelter BO (2016) Efficacy and safety of tau-aggregation inhibitor therapy in patients with mild or moderate Alzheimer's disease: A randomised, controlled, double-blind, parallel-arm, phase 3 trial. *Lancet* **388**, 2873-2884.

[58] Li C, Götz J (2017) Tau-based therapies in neurodegeneration: Opportunities and challenges. *Nat Rev Drug Discov* **16**, 863.

[59] Davis DG, Schmitt FA, Wekstein DR, Markesbery WR (1999) Alzheimer neuropathologic alterations in aged cognitively normal subjects. *J Neuropathol Exp Neurol* **58**, 376-388.

[60] Edison P, Archer HA, Hinz R, Hammers A, Pavese N, Tai YF, Hotton G, Cutler D, Fox N, Kennedy A, Rossor M, Brooks DJ (2007). Amyloid, hypometabolism, and cognition in Alzheimer disease: An [11C] PIB and [18F] FDG PET study. *Neurology* **68**, 501-508.

[61] Li Y, Rinne JO, Mosconi L, Pirraglia E, Rusinek H, DeSanti S, Kemppainen N, Någren K, Kim BC, Tsui W, De Leon MJ (2008) Regional analysis of FDG and PIB-PET images in normal aging, mild cognitive impairment, and Alzheimer's disease. *Eur J Nucl Med Mol Imaging* **35**, 2169-2181.

[62] Fagan AM, Mintun MA, Shah AR, Aldea P, Roe CM, Mach RH, Marcus D, Morris JC, Holtzman DM (2009) Cerebrospinal fluid tau and ptau181 increase with cortical amyloid deposition in cognitively normal individuals: Implications for future clinical trials of Alzheimer's disease. *EMBO Mol Med* **1**, 371-380.

[63] Price JL, McKeel DW, Buckles VD, Roe CM, Xiong C, Grundman M, Hansen LA, Petersen RC, Parisi JE, Dickson DW, Smith CD (2009) Neuropathology of nondemented aging: Presumptive evidence for preclinical Alzheimer disease. *Neurobiol Aging* **30**, 1026-1036.

[64] Chételat G, La Joie R, Villain N, Perrotin A, de La Sayette V, Eustache F, Vandenberghe R (2013) Amyloid imaging in cognitively normal individuals, at-risk populations and preclinical Alzheimer's disease. *Neuroimage Clin* **2**, 356-365.

[65] Janson J, Laedtke T, Parisi JE, O'Brien P, Petersen RC, Butler PC (2004) Increased risk of type 2 diabetes in Alzheimer disease. *Diabetes* **53**, 474-481.

[66] Do K, Laing BT, Landry T, Bunner W, Mersaud N, Matsubara T, Li P, Yuan Y, Lu Q, Huang H (2018) The effects of exercise on hypothalamic neurodegeneration of Alzheimer's disease mouse model. *PloS One* **13**, e0190205.

[67] Thal DR, Rüb U, Orantes M, Braak H (2002) Phases of Aβ-deposition in the human brain and its relevance for the development of AD. *Neurology* **58**, 1791-1800.

[68] Macauley SL, Stanley M, Caesar EE, Yamada SA, Raichle ME, Perez R, Mahan TE, Sutphen CL, Holtzman DM (2015) Hyperglycemia modulates extracellular amyloid-β concentrations and neuronal activity in vivo. *J Clin Invest* **125**, 2463-2467.

[69] Devi L, Alldred MJ, Ginsberg SD, Ohno M (2012) Mechanisms underlying insulin deficiency-induced acceleration of β-amyloidosis in a mouse model of Alzheimer's disease. *PLoS One* **7**, e32792.

[70] Lambert MP, Barlow AK, Chromy BA, Edwards C, Freed R, Liosatos M, Morgan TE, Rozovsky I, Trommer B, Viola KL, Wals P, Zhang C, Finch CE, Krafft GA, Klein WL, Prusiner SB (1998) Diffusible, nonfibrillar ligands derived from Aβ 1– 42 are potent central nervous system neurotoxins. *Neurobiology* **95**, 6448-6453.

[71] Fitzjohn SM, Morton RA, Kuenzi F, Rosahl TW, Shearman M, Lewis H, Smith D, Reynolds DS, Davies CH, Collingridge GL, Seabrook GR (2001) Age-related impairment of synaptic transmission but normal long-term potentiation in transgenic mice that overexpress the human APP695SWE mutant form of amyloid precursor protein. *J Neurosci* **21**, 4691-4698.

[72] Shankar GM, Li S, Mehta TH, Garcia-Munoz A, Shepardson NE, Smith I, Brett FM, Farrell MA, Rowan MJ, Lemere C, Regan CM, Walsh DM, Sabatini BL, Selkoe DJ, (2008) Amyloid-beta protein dimers isolated directly from Alzheimer's brains impair synaptic plasticity and memory. *Nat Med* **14**, 837-842.

[73] Zhao WQ, De Felice FG, Fernandez S, Chen H, Lambert MP, Quon MJ, Krafft GA, Klein WL (2008) Amyloid beta oligomers induce impairment of neuronal insulin receptors. *FASEB J* **22**, 246-260.

[74] Nekrep N, Wang J, Miyatsuka T, German MS, Pedersen RA, Rubenstein JL, German MS (2008) Signals from the neural crest regulate beta-cell mass in the pancreas. *Development* **135**, 2151-2160.

[75] Chen X, Garelick MG, Wang H, Lil V, Athos J, Storm DR (2005) PI3 kinase signaling is required for retrieval and extinction of contextual memory. *Nat Neurosci* **8**, 925-931.

[76] English JD, Sweatt JD (1996) Activation of p42 mitogen-activated protein kinase in hippocampal long term potentiation. *J Biol Chem* **271**, 24329-24332.

[77] Karpova A, Sanna PP, Behnisch T (2006) Involvement of multiple phosphatidylinositol 3-kinase-dependent pathways in the persistence of late-phase long term potentiation expression. *Neuroscience* **137**, 833-841.

[78] Kelly Á, Lynch M (2000) Long-term potentiation in dentate gyrus of the rat is inhibited by the phosphoinositide 3–kinase inhibitor, wortmannin. *Neuropharmacology* **39**, 643-651.

[79] Mizuno M, Yamada K, Takei N, Tran MH, He J, Nakajima A, Nawa H, Nabeshima T (2003) Phosphatidylinositol 3-kinase: A molecule mediating BDNF-dependent spatial memory formation. *Mol Psychiatry* **8**, 217-224.

[80] Raymond CR, Redman SJ (2002) Different calcium sources are narrowly tuned to the induction of different forms of LTP. *J Neurophysiol* **88**, 249-255.

[81] Thomas GM, Huganir RL (2004) MAPK cascade signalling and synaptic plasticity. *Nat Rev Neurosci* **5**, 173-183.

[82] Zhao W, Chen H, Xu H, Moore E, Meiri N, Quon MJ, Alkon DL (1999) Brain insulin receptors and spatial memory. Correlated changes in gene expression, tyrosine phosphorylation, and signaling molecules in the hippocampus of water maze trained rats. *J Biol Chem* **274**, 34893-34902.

[83] Kim EK, Choi EJ (2010) Pathological roles of MAPK signaling pathways in human diseases. *Biochem Biophys Acta* **1802**, 396-405.

[84] Son Y, Cheong YK, Kim NH, Chung HT, Kang DG, Pae HO (2011) Mitogen-activated protein kinases and reactive oxygen species: How can ROS activate MAPK pathways? *J Signal Transduct* **2011**, 792639.

[85] Janelsins MC, Mastrangelo MA, Oddo S, LaFerla FM, Federoff HJ, Bowers WJ (2005) Early correlation of microglial activation with enhanced tumor necrosis factor-alpha and monocyte chemoattractant protein-1 expression specifically within the entorhinal cortex of triple transgenic Alzheimer's disease mice. *J Neuroinflammation* **2**, 23.

[86] Janelsins MC, Mastrangelo MA, Park KM, Sudol KL, Narrow WC, Oddo S, LaFerla FM, Callahan LM, Federoff HJ, Bowers WJ (2008) Chronic neuron-specific tumor necrosis factor-alpha expression enhances the local inflammatory environment ultimately leading to neuronal death in 3xTg-AD mice. *Am J Pathol* **173**, 1768-1782.

[87] Olabarria M, Noristani HN, Verkhratsky A, Rodríguez JJ (2010) Concomitant astroglial atrophy and astrogliosis in a triple transgenic animal model of Alzheimer's disease. *Glia* **58**, 831-838.

[88] Rodriguez JJ, Witton J, Olabarria M, Noristani HN, Verkhratsky A (2011) Increase in the density of resting microglia precedes neuritic plaque formation and microglial activation in a transgenic model of Alzheimer's disease. *Cell Death Dis* **1**, e1.

[89] Townsend, M, Mehta T, Selkoe DJ (2007) Soluble Aβ inhibits specific signal transduction cascades common to the insulin receptor pathway. *J Biol Chem* **282**, 33305-33312.

[90] Savage MJ, Lin YG, Ciallella JR, Flood DG, Scott RW (2002) Activation of c-Jun N-terminal kinase and p38 in an Alzheimer's disease model is associated with amyloid deposition. *J Neurosci* **22**, 3376-3385.

[91] Ghasemi R, Zarifkar A, Rastegar K, Maghsoudi N, Moosavi M (2014) Repeated intra-hippocampal injection of beta-amyloid 25–35 induces a reproducible impairment of learning and memory: Considering caspase-3 and MAPKs activity. *Eur J Pharmacol* **726**, 33-40.

[92] Chen Y, Liang Z, Tian Z, Blanchard J, Dai C-L, Chalbot S, Iqbal K, Liu F, Gong C-X (2014) Intracerebroventricular streptozotocin exacerbates Alzheimer-like changes of 3xTg-AD mice. *Mol Neurobiol* **49**, 547-562.

[93] Kanety H, Feinstein R, Papa MZ, Hemi R, Karasik A (1995) Tumor necrosis factor α-induced phosphorylation of insulin receptor substrate-1 (IRS-1) Possible mechanism for suppression of insulin-stimulated tyrosine phosphorylation of IRS-1. *J Biol Chem* **270**, 23780-23784.

[94] Hotamisligil GS, Peraldi P, Budavari A, Ellis R, White MF, Spiegelman BM (1996) IRS-1-mediated inhibition of insulin receptor tyrosine kinase activity in TNF-α-and obesity-induced insulin resistance. *Science* **271**, 665-670.

[95] Rui L, Aguirre V, Kim JK, Shulman GI, Lee A, Corbould A, Dunaif A, White MF (2001) Insulin/IGF-1 and TNF-α stimulate phosphorylation of IRS-1 at inhibitory Ser 307 via distinct pathways. *J Clin Invest* **107**, 181-89.

[96] Chen Y, Zhao Y, Dai CL, Liang Z, Run X, Iqbal K, Liu F, Gong CX (2014) Intranasal insulin restores insulin signaling, increases synaptic proteins, and reduces Aβ level and microglia activation in the brains of 3xTg-AD mice. *Exp Neurol* **261**, 610-619.

[97] Devaskar SU, Giddings SJ, Rajakumar PA, Carnaghi LR, Menon RK, Zahm DS (1994) Insulin gene expression and insulin synthesis in mammalian neuronal cells. *J Biol Chem* **269**, 8445-8454.

[98] Schechter R, Holtzclaw L, Sadiq F, Kahn A, Devaskar S (1988) Insulin synthesis by isolated rabbit neurons. *Endocrinology* **123**, 505-513.

[99] Heras-Sandoval D, Ferrera P, Arias C (2012) Amyloid-β protein modulates insulin signaling in presynaptic terminals. *Neurochem Res* **37**, 1879-1885.

[100] Carney JM, Carney AM (1994) Role of protein oxidation in aging and in age-associated neurodegenerative diseases. *Life Sci* **55**, 2097-2103.

[101] Emerit J, Edeas M, Bricaire F (2004) Neurodegenerative diseases and oxidative stress. *Biomed Pharmacother* **58**, 39-46.

[102] Hawkins PT, Stephens LR (2015) PI3K signalling in inflammation. *Biochim Biophys Acta* **1851**, 882-897.

[103] Park J, Min JS, Kim B, Chae UB, Yun JW, Choi MS, Kong IK, Chang KT, Lee DS (2015) Mitochondrial ROS govern the LPS-induced pro-inflammatory response in microglia cells by regulating MAPK and NF-κB pathways. *Neurosci Lett* **584**, 191-196.

[104] Kim HG, Shrestha B, Lim SY, Yoon DH, Chang WC, Shin DJ, Han SK, Park SM, Park JH, Park HI, Sung JM (2006) Cordycepin inhibits lipopolysaccharide-induced inflammation by the suppression of NF-κB through Akt and p38 inhibition in RAW 264.7 macrophage cells. *Eur J Pharm* **545**, 192-199.

[105] Claxton A, Baker LD, Hanson A, Trittschuh EH, Cholerton B, Morgan A, Callaghan M, Arbuckle M, Behl C, Craft, S (2015) Long-acting intranasal insulin detemir improves cognition for adults with mild cognitive impairment or early-stage Alzheimer's disease dementia. *J Alzheimers Dis* **44**, 897-906.

[106] Woodgett JR (1990) Molecular cloning and expression of glycogen synthase kinase-3/factor A. *EMBO J* **9**, 2431-2438.

[107] Hoeflich KP, Luo J, Rubie EA, Tsao MS, Jin O, Woodgett JR (2000) Requirement for glycogen synthase kinase-3beta in cell survival and NF-kappaB activation. *Nature* **406**, 86-90.

[108] Ougolkov AV, Bone ND, Fernandez-Zapico ME, Kay NE, Billadeau DD, O'Brien S, Rai KR (2007) Inhibition of glycogen synthase kinase-3 activity leads to epigenetic silencing of nuclear factor kappaB target genes and induction of apoptosis in chronic lymphocytic leukemia B cells. *Blood* **110**, 735-742.

[109] Takada Y, Fang X, Jamaluddin MS, Boyd DD, Aggarwal BB (2004) Genetic deletion of glycogen synthase kinase-3beta abrogates activation of IkappaBalpha kinase, JNK, Akt, and p44/p42 MAPK but potentiates apoptosis induced by tumor necrosis factor. *J Biol Chem* **279**, 39541-39554.

[110] Carmichael J, Sugars KL, Bao YP, Rubinsztein DC (2002) Glycogen synthase kinase-3beta inhibitors prevent cellular polyglutamine toxicity caused by the Huntington's disease mutation. *J Biol Chem* **277**, 33791-33798.

[111] Jin N, Kovács AD, Sui Z, Dewhurst S, Maggirwar SB (2005) Opposite effects of lithium and valproic acid on trophic factor deprivation-induced glycogen synthase kinase-3 activation, c-Jun expression and neuronal cell death. *Neuropharm* **48**, 576-583.

[112] Maggirwar SB, Tong N, Ramirez S, Gelbard HA, Dewhurst S (2002) HIV-1 Tat-mediated activation of glycogen synthase kinase-3β contributes to tat-mediated neurotoxicity. *J Neurochem* **73**, 578-586.

[113] Pap M, Cooper GM (1998) Role of glycogen synthase kinase-3 in the phosphatidylinositol 3-Kinase/Akt cell survival pathway. *J Biol Chem* **273**, 19929-19932.

[114] Tong N, Sanchez JF, Maggirwar SB, Ramirez SH, Guo H, Dewhurst S, Gelbard HA (2001) Activation of glycogen synthase kinase 3 beta (GSK-3β) by platelet activating factor mediates migration and cell death in cerebellar granule neurons. *Eur J Neurosci* **13**, 1913-1922.

[115] Sato N, Meijer L, Skaltsounis L, Greengard P, Brivanlou AH (2004) Maintenance of pluripotency in human and mouse embryonic stem cells through activation of Wnt signaling by a pharmacological GSK-3-specific inhibitor. *Nat Med* **10**, 55-63.

[116] Tseng AS, Engel FB, Keating MTT (2006) The GSK-3 inhibitor BIO promotes proliferation in mammalian cardiomyocytes. *Chem Biol* **13**, 957-963.

[117] Akiyama H, Shin RW, Uchida C, Kitamoto T, Uchida T (2005) Pin1 promotes production of Alzheimer's amyloid β from β-cleaved amyloid precursor protein. *Biochem Biophys Res Commun* **336**, 521-529.

[118] Bayatti N, Zschocke J, Behl C (2003) Brain region-specific neuroprotective action and signaling of corticotropin-releasing hormone in primary neurons. *Endocrinology* **144**, 4051-4060.

[119] Ryder J, Su Y, Liu F, Li B, Zhou Y, Ni B (2003) Divergent roles of GSK3 and CDK5 in APP processing. *Biochem Biophys Res Commun* **312**, 922-929.

[120] Su Y, Ryder J, Li B, Wu X, Fox N, Solenberg P, Brune K, Paul S, Zhou Y, Liu F, Ni B (2004) Lithium, a common drug for bipolar disorder treatment, regulates amyloid-β precursor protein processing. *Biochemistry* **43**, 6899-6908.

[121] Jope RS, Yuskaitis CJ, Beurel E (2007) Glycogen synthase kinase-3 (GSK3): Inflammation, diseases, and therapeutics. *Neurochem Res* **32**, 577-595.

[122] Lipton SA (2008) NMDA receptor activity regulates transcription of antioxidant pathways. *Nat Neurosci* **11**, 381-382.

[123] Hong M, Lee VM (1997) Insulin and insulin-like growth factor-1 regulate tau phosphorylation in cultured human neurons. *J Biol Chem* **272**, 19547-19553.

[124] Ishiguro K, Shiratsuchi A, Sato S, Omori A, Arioka M, Kobayashi S, Uchida T, Imahori K (1993) Glycogen synthase kinase 3β is identical to tau protein kinase I generating several epitopes of paired helical filaments. *FEBS Lett* **325**, 167-172.

[125] Bingham EM, Hopkins D, Smith D, Pernet A, Hallett W, Reed L, Marsden PK, Amiel SA (2002) The role of insulin in human brain glucose metabolism: An 18Fluoro-deoxyglucose positron emission tomography study. *Diabetes* **51**, 3384-3390.

[126] Doyle P, Cusin I, Rohner-Jeanrenaud F, Jeanrenaud B (1995) Four-day hyperinsulinemia in euglycemic conditions alters local cerebral glucose utilization in specific brain nuclei of freely moving rats. *Brain Res* **684**, 47-55.

[127] Fisher SJ, Bruning JC, Lannon S, Kahn CR (2005) Insulin signaling in the central nervous system is critical for the normal sympathoadrenal response to hypoglycemia. *Diabetes* **54**, 1447-1451.

[128] Grillo CA, Piroli GG, Hendry RM, Reagan LP (2009) Insulin-stimulated translocation of GLUT4 to the plasma membrane in rat hippocampus is PI3-kinase dependent. *Brain Res* **1296**, 35-45.

[129] Uemura E, Greenlee HW (2006) Insulin regulates neuronal glucose uptake by promoting translocation of glucose transporter GLUT3. *Exp Neurol* **198**, 48-53.

[130] Gold PE (2005) Glucose and age-related changes in memory. *Neurobiol Aging* **26**(Suppl 1), 60-64.

[131] McNay EC, Fries TM, Gold PE (2000) Decreases in rat extracellular hippocampal glucose concentration associated with cognitive demand during a spatial task. *Proc Natl Acad Sci U S A* **97**, 2881-2885.

[132] McNay EC, Gold PE (2001) Age-related differences in hippocampal extracellular fluid glucose concentration during behavioral testing and following systemic glucose administration. *J Gerontol A Biol Sci Med Sci* **56**, 66-71.

[133] Simpson IA, Chundu KR, Davies-Hill T, Honer WG, Davies P (1994) Decreased concentrations of GLUT1 and GLUT3 glucose transporters in the brains of patients with Alzheimer's disease. *Ann Neurol* **35**, 546-551.

[134] Liu Y, Liu F, Grundke-Iqbal I, Iqbal K, Gong C-X (2009) Brain glucose transporters, O-GlcNAcylation and phosphorylation of tau in diabetes and Alzheimer's disease. *J Neurochem* **111**, 242-249.

[135] Prapong T, Buss J, Hsu WH, Heine P, West Greenlee H, Uemura E (2002) Amyloid beta-peptide decreases neuronal glucose uptake despite causing increase in GLUT3 mRNA transcription and GLUT3 translocation to the plasma membrane. *Exp Neurol* **174**, 253-258.

[136] Simpson IA, Cushman SW (1986) Hormonal regulation of mammalian glucose transport. *Annu Rev Biochem* **55**, 1059-1089.

[137] Apelt J, Mehlhorn G, Schliebs R (1999) Insulin-sensitive GLUT4 glucose transporters are colocalized with GLUT3-expressing cells and demonstrate a chemically distinct neuron-specific localization in rat brain. *J Neurosci Res* **57**, 693-705.

[138] El Messari S, Aït-Ikhlef A, Ambroise DH, Penicaud L, Arluison M (2002) Expression of insulin-responsive glucose transporter GLUT4 mRNA in the rat brain and spinal cord: An in situ hybridization study. *J Chem Neuroanat* **24**, 225-242.

[139] Vannucci SJ, Koehler-Stec EM, Li K, Reynolds TH, Clark R, Simpson I (1998) GLUT4 glucose transporter expression in rodent brain: Effect of diabetes. *Brain Res* **797**, 1-11.

[140] Havrankova J, Schmechel D, Roth J, Brownstein M (1978) Identification of insulin in rat brain. *Proc Natl Acad Sci U S A* **75**, 5737-5741.

[141] Heidenreich KA, Zahniser NR, Berhanu P, Brandenburg D, Olefsky JM (1983) Structural differences between insulin receptors in the brain and peripheral target tissues. *J Biol Chem* **258**, 8527-8530.

[142] Marks JL, Porte D, Stahl WL, Baskin DG (1990) Localization of insulin receptor mRNA in rat brain by in situ hybridization. *Endocrinology* **127**, 3234-3236.

[143] Unger JW, Livingston JN, Moss AM (1991) Insulin receptors in the central nervous system: Localization, signalling mechanisms and functional aspects. *Prog Neurobiol* **36**, 343-362.

[144] Benomar Y, Naour N, Aubourg A, Bailleux V, Gertler A, Djiane J, Guerre-Millo M, Taouis M (2006) Insulin and leptin induce Glut4 plasma membrane translocation and glucose uptake in a human neuronal cell line by a phosphatidylinositol 3-kinase-dependent mechanism. *Endocrinology* **147**, 2550-2556.

[145] Fernando RN, Albiston AL, Chai SY (2008) The insulin-regulated aminopeptidase IRAP is colocalised with GLUT4 in the mouse hippocampus–potential role in modulation of glucose uptake in neurones? *Eur J Neurosci* **28**, 588-598.

[146] Imamura T, Huang J, Usui I, Satoh H, Bever J, Olefsky JM (2003) Insulin-induced GLUT4 translocation involves protein kinase C- mediated functional coupling between Rab4 and the motor protein kinesin. *Mol Cell Biol* **23**, 4892-4900.

[147] Roher N, Samokhvalov V, Díaz M, MacKenzie S, Klip A, Planas JV (2008) The proinflammatory cytokine tumor necrosis factor-α increases the amount of glucose transporter-4 at the surface of muscle cells independently of changes in interleukin-6. *Endocrinology* **149**, 1880-1889.

[148] Burcelin R, Crivelli V, Perrin C, Da Costa A, Mu J, Kahn BB, Birnbaum MJ, Kahn CR, Vollenweider P, Thorens B (2003) GLUT4, AMP kinase, but not the insulin receptor, are required for hepatoportal glucose sensor-stimulated muscle glucose utilization. *J Clin Invest* **111**, 1555-1562.

[149] Lawrence JT, Birnbaum MJ (2001) ADP-ribosylation factor 6 delineates separate pathways used by endothelin 1 and insulin for stimulating glucose uptake in 3T3-L1 adipocytes. *Mol Cell Biol* **21**, 5276-5285.